HONG KONG OBSERVATORY

Technical Note (Local) No. 82

A Random-Walk Particle Dispersion Model for Radiological Accident Consequence Assessment

by

H.Y. Lam, S.W. Li and P.Y. Yeung

Published September 2005

Prepared by

Hong Kong Observatory
134A Nathan Road
Kowloon
Hong Kong

551.510.7

摘要

本報告描述一套由香港天文台所發展用於輻射事故後果評價的隨機位移粒子擴散模式的組成部分及其模擬結果。

粒子擴散模式由四個模組組合而成，它們是：氣象模組、擴散模組、劑量及防護措施模組和介面及控制模組。與二維高斯煙羽模式不同，粒子擴散模式利用含有隨機位移方法來模擬湍流擴散，把釋放的物質分成眾多等值放射性的虛構粒子，利用實時風站資料和數值模擬預測的二維風場，加上降水和大氣穩定度與及地形資料，推算未來 24 小時的三維風場，用來估計粒子的移動及分佈情況。因此，該模式亦能計算釋出物質在大氣的濃度和地面沉降量，與及公眾接受到的輻射劑量。粒子擴散模式模擬煙羽的結果亦和現存的業務事故後果評價系統的模擬結果作了比對，結果顯示兩套模式在不同的大氣穩定度下，煙羽中央線的大氣濃度和地面沉降在香港境內差別一般不逾一個數量級，而煙羽的闊度亦相若。總的來說，粒子擴散模式可為評估輻射事故的影響提供有用參考。

Abstract

This report describes the components and the simulation results of a Random-Walk Particle Dispersion Model for Radiological Accident Consequence Assessment developed by the Hong Kong Observatory.

The Particle Dispersion Model (PDM) is composed of four modules, namely the Meteorological Module, the Dispersion Module, the Dose and Protective Action Module and the Interface and Control Module. Unlike the 2-dimensional Gaussian plume model, PDM employs a random-walk particle approach which splits the released material into numerous fictitious particles with equal amount of radioactivity. By using real-time wind information, 2-dimensional wind field forecasts from numerical weather prediction system, rainfall and atmospheric stability, as well as terrain information, the PDM generates 3-dimensional wind fields for the next 24-hours and estimates the movement and distribution of the particles. Hence, it is capable of computing the air concentration and ground deposition of the radioactive material released, as well as dosage to the public due to radioactivity exposure. Comparison of results between the PDM and the existing operational Accident Consequence Assessment System (ACAS) under different atmospheric stabilities indicate that the air concentration and ground deposition generally differ at most by about one order of magnitude along the centreline of the simulated dispersion plumes, and the plume widths are similar for both models. It is concluded that the PDM can serve as a useful reference for assessing the impact in the event of a radiological accident.

CONTENTS

LIST OF TABLES

LIST OF FIGURES

1. Introduction

The Hong Kong Observatory (HKO) operates an Accident Consequence Assessment System (ACAS) for assessing the radiological consequence in the event of a release from the Guangdong Nuclear Power Station (GNPS) / Lingao Nuclear Power Station (LNPS) at Daya Bay. ACAS is a computer-based system capable of acquiring real-time meteorological information from automatic and manned weather stations. Using these meteorological data and available or assumed source term information, ACAS simulates the dispersion of the released radioactive material. It also predicts the radiation dose to the public over the territory of Hong Kong (PLG, 1991).

In operation since 1992, ACAS employs a 2-dimensional segmented Gaussian dispersion model. Specifically, the movement of the radioactive plume follows a 2-dimensional wind field interpolated from surface observations. In forecasting the plume track, the program extrapolates the latest wind information by persistence for predicting plume movement in the short term. As output, ACAS produces estimates of air concentration and ground deposition, as well as various doses at fixed forecast times after the release from a fixed source location.

In recent years, HKO had taken steps to improve, both in quality and quantity, the collection of real-time meteorological data as well as generation of numerical weather prediction products. The Operational Regional Spectral Model (ORSM) operated by HKO provides mesoscale forecasts of horizontal wind fields, cloud and rainfall for areas over southeastern Asia and western Pacific for up to 72 hours ahead (Lam and Yeung, 2003). At the same time, as models are capable of providing a more realistic dispersion simulation over complex terrain, 3-dimensional wind field and particle models are becoming popular in dispersion simulation systems (Sherman, 1978; Ley, 1982; Imai *et al*., 1985; Etling *et al*., 1986; Thomson, 1986; Tian and Wang, 2001; Ross *et al*., 1988; Ross and Fox, 1991; and Venkatesan *et al*., 1997).

As a continuing effort to improve its capability in accident consequence assessment, HKO has developed a dispersion model using a random-walk particle approach to simulate the movement of radionuclides. The Particle Dispersion Model (PDM) is a 3-dimensional system, making use of available meteorological information with improved quality, to calculate the dispersion of radioactive plumes in the early phase of release and the associated doses to the public. It is capable of estimating air concentration and ground deposition of radionuclides at a better temporal resolution than ACAS (i.e. every hour in PDM as opposed to at least every 3 hours in ACAS). Moreover, PDM allows flexible selection of the source release location. The aim of the present study is to assess PDM by comparing its simulation results against those obtained by ACAS.

2. Structure of the Particle Dispersion Model

PDM consists of four modules:

a. Meteorological Module;
b. Dispersion Module;
c. Dose and Protective Action Module; and
d. Interface and Control Module.

The function of the Meteorological Module is to diagnose a 3-dimensional wind field using available weather and terrain information. The generated wind field then drives the Dispersion Module to simulate plume movement and dispersion and to generate air concentration and ground deposition fields. Subsequently, these fields are used in the Dose and Protective Action Module to calculate the dose to the public and the possible dose reduction due to implementation of countermeasures. The Interface and Control Module ingests data required as input for model simulation and presents model outputs for reference by emergency response personnel.

2.1 Meteorological Module

Within PDM, the Meteorological Module processes weather data from various sources and generates wind fields in the format acceptable by the Dispersion Module for the simulation of plume movement and dispersion.

The Meteorological Module employs a diagnostic wind field model based on the "variational method" (details in Appendix I). It simulates 3-dimensional non-divergent, or mass conservative, flows around the complex terrain over Hong Kong and its vicinity, taking into account thermodynamics forcing. Figure 1 is a block diagram showing stages of data processing in the Module. The domain size, grid setting and terrain information used are shown in Appendix II.

In contrast, the wind field model of ACAS is 2-dimensional and employs the Barnes Scheme interpolation algorithm. The Gaussian model adopted by ACAS assumes that wind speed and turbulence are vertically homogeneous. The wind field generated is not mass conservative because the effect of terrain is not included.

In order to simulate the 3-dimensional wind fields over the model domain, hourly meteorological data is needed. Three types of meteorological data are ingested into the Meteorological Module:

(a) wind data from automatic weather stations over Hong Kong and those around Daya Bay provided by the Guangdong authority for wind field analysis;
(b) synoptic reports from HKIA for atmospheric stability computation; and
(c) 9 x 9 grid point data (20 km horizontal resolution) from ORSM near surface and 850 hPa level wind and cloud analysis for the next 24 hours.

The above surface and 850 hPa level data are interpolated by Cressman weighting into a 33 x 33 grid with a horizontal resolution of 5 km over the whole domain. The fields are updated when new data are available from synoptic observations and automatic weather stations at hourly intervals, as well as from ORSM at 3-hourly intervals. Grid point winds at intermediate vertical layers between the surface and the model top are obtained by linear interpolation in proportion to the depth of each layer. This pre-processed wind field is then analyzed by the variational method to generate a mass-conserved 3-dimensional wind field with vertical wind components for the current and the next 24 hours. Besides the wind fields, hourly stability categories for the same period are also calculated for use by the Dispersion Module.

The algorithm and computer coding documented in Cheng *et al*. (1989) are employed to calculate the stability categories. The algorithm estimates the stability according to insolation, cloud coverage, cloud ceiling height and wind speed. Insolation is based on sunrise and sunset times, as well as solar altitude which depend on the time of the day and the day of the year. In PDM, the stability categories for the synoptic station at the Hong Kong International Airport (HKIA) are taken to represent the whole calculation domain. The actual cloud cover, ceiling height and wind speed are extracted from the observations at HKIA. The forecast cloud cover and winds are linearly interpolated from ORSM's hourly 850 hPa cloud and surface wind forecasts respectively to provide values at HKIA.

The computed hourly stability categories at HKIA in 2003 are shown in Table 1. It can be seen that the atmospheric stability is mostly neutral (Category D), while extremely stable (Category G) and extremely unstable cases (Category A) only constitute small percentage of 2.3% and 1.0% respectively.

2.2 Dispersion Module

The Dispersion Module takes in the wind fields and atmospheric stability obtained from the Meteorological Module, as well as rainfall and release source term information. It then calculates the instantaneous and time integrated air concentration and ground deposition due to radioactive release using a random-walk particle approach. The time integrated quantities are summed up to 3, 6, 12 and 24 hours. Outputs from the module are to be used by the Dose and Protective Action Module to estimate the dose to the public.

The main component of this Module is a random-walk particle dispersion model, which is similar to the JAERI's SPEEDI. Details of the random-walk particle approach are described in Appendix III. Besides simple translation and dispersion of the radioactive material, the Dispersion Module also includes schemes to simulate radioactive decay, and dry and wet deposition. The schemes are described in Appendices IV and V respectively. Figure 2 is a block diagram showing stages of data processing in the Module. Compared with the existing ACAS, the PDM has the following advantages:

(a) providing finer structure of the plume in both horizontal and vertical directions as it is driven by 3-dimensional wind fields;
(b) incorporating terrain effects;
(c) allowing flexible selection of source release of up to 8 radionuclides;
(d) allowing release source of up to 4 locations at different heights; and
(e) providing instantaneous air concentration in addition to time integrated ones.

Figure 3 shows a sample output of the 3-dimensional dispersion of particles over terrain.

2.3 Dose and Protective Action Module

The Dose and Protective Action Module takes grid-point values of air concentration and ground deposition obtained from the Dispersion Module as input estimate various doses received by the public. These doses include the whole body dose, thyroid dose, lung dose and skin dose. Dose reduction due to implementation of countermeasures is also estimated.

For dosage calculation, potential routes through which human bodies may be exposed to radioativity, and hence accumulate dose, are called 'exposure pathways'. The pathways are:

(a) external exposure to the radioactive plume;
(b) internal exposure due to inhalation of plume;
(c) external exposure to the radionuclides deposited on the ground; and
(d) internal exposure due to inhalation of re-suspended radionuclides deposited on the ground.

As PDM is primarily concerned with the early phase of an accident when the plume is in the vicinity of Hong Kong, the last exposure pathway, i.e. (d), can normally be neglected in view of its insignificant contribution to the total dose compared to the other exposure pathways.

The dose coefficients and estimation of external and internal doses will be described in Appendix VI. Details of possible protection actions in the event of a nuclear power station accident are given in Appendix VII.

2.4 Interface and Control Module

Graphical user interfaces (GUIs) for submitting PDM simulation and outputting results have been developed. The GUIs are written in Visual Basic and are user-friendly. The input interface takes in the necessary parameters for the wind field simulations. The user can input information including locations of source, release start time and duration, release height, and the source term such as release rate of each radionuclides. He/she can also switch on or off the terrain effect as well as the countermeasures to be implemented in the simulation. When the simulation is completed, the output file being large in size is converted into easy-to-read graphics to facilitate interpretation. The output GUI gives the user freedom to select the products to be displayed. The GUI also has a zoom-in function which enables the user to enlarge the output plots for detailed investigation.

3. Comparison of Simulation Results between PDM and ACAS

To assess the performance of PDM, simulation results of various quantities are compared with the existing ACAS under different atmospheric conditions.

Although a number of radionuclides may be released in a reactor accident, only a few are of significance to the dose received by people off-site. These are isotopes of iodine (I-131, I-132 and I-133) and caesium (Cs-134 and Cs-137). Apart from inert gases, I-131 is the one of the major isotopes normally released in nuclear accidents, e.g. the Three Mile Island and Chernobyl accidents. In this comparison exercise, the source was taken to be I-131 at the source. A nominal rate of 1 Bq/s for 3 hours was assumed. The comparison results should be applicable to the other radionuclides as the effect of radioactive decay of different radionuclides should be small during the plume phase. As regards meteorological conditions, the prevailing winds were assumed constant from the northeast (045°) with no rainfall. Simulations were performed under different atmospheric stabilities from Category A (extremely unstable) to Category G (extremely stable) for low wind speed (2 m/s). For higher wind speeds, the atmospheric stability will normally be neutral because of mixing. Simulations were thus only performed for Category D (neutral) and for a higher wind speed (5 m/s).

In the comparison, the simulated dispersion plumes were analyzed in terms of the 24-hour integrated air concentration, ground deposition and various doses received by the human body. Values along the centreline of the plume downwind as well as over the plume spread were studied. Table 2 summarizes the input conditions for the simulation and the output parameters studied in the present comparison.

3.1 Along Centreline

A nuclear release is very similar to smoke release from a stack. Radioactive material is transported downwind by the prevailing flow and is dispersed due to turbulence. As the prevailing flow is usually one or two orders of magnitude higher than that of turbulence, i.e. m/s versus cm/s, the effect of this is that the material propagates in a plume shape with concentration decreasing away from the source. Away from the centreline of the plume, the concentration of the radioactive material decreases. As such, values along the centreline are usually investigated so that the worst case scenario can be considered.

In this comparison, simulation results obtained from PDM are compared side-by-side to those from the ACAS for air concentration, ground deposition, whole body dose, thyroid dose, lung dose and skin dose.

In comparing the plume shape, it may appear at first sight that the plumes simulated by ACAS are generally shorter than those by PDM. This is actually related to the restrictions in the plotting routine of ACAS whereby values beyond the preset colour scale are not plotted. Despite this, the comparison can still be performed as ACAS does provide simulated values beyond the "plotted plume".

24-hour integrated quantities on the centreline at 6 different downwind distances from source, i.e. 15, 25, 35, 45.5, 55.5 and 70 km, are compared and tabulated in Table 3 to 8. For ease of comparison, although simulations are performed under different atmospheric stabilities for low wind speed, only the results for stability Categories B, D and F will be presented here. This is because, as discussed in Section 2.1, the occurrence of stability Categories A and G altogether constitute only 3.3% of the time in a year. It is also observed in the results that the plume characteristic of Category C (E) lies between those of Categories B (D) and D (F) and as such, Category C (E) results are not presented. As mentioned before, comparison was only performed for category D under well mixed conditions with a moderate wind speed (5 m/s).

3.1.1 Air Concentrations

In the present comparison, the air concentration is defined as the 24-hour integrated value at the lowest layer of the model. Table 3 shows the results of simulated air concentration at different downwind distances along the plume centreline under various atmospheric stability categories and wind speeds. The results indicate that the difference in air concentration between ACAS and PDM is within a factor of 20 despite of the intrinsic difference between the two models in handling dispersion (particle approach in the PDM versus Gaussian dispersion in the ACAS) and in stability determination.

(a) Light Wind Conditions (2 m/s)

Under the very unstable conditions of stability Category B, the centreline air concentration simulated by the PDM is about 3 to 4 times higher than those in ACAS, but with a similar rate of decrease with distance beyond 15 km downwind of the source (Figure 4a). This implies that both models bear similar dispersion characteristics with PDM being more conservative. For the neutral case (Figure 4b), i.e. Category D, the values over the urban areas of Hong Kong differ by less than 1.5 times. For Category F, the difference is about 7 times.

Nearer to the source (within 20 km), PDM gives a lower air concentration than ACAS for Categories D and F (i.e. neutral and very stable conditions). The air concentration is, however, higher for longer distances. This is associated with a slower rate of decrease in the simulated air concentration with distance for PDM (Figure 4b-c). One reason for this is that particles disperse less in the horizontal direction in PDM and as a result are more concentrated near the plume centre. This will be discussed in more detail in Section 3.2.

(a) Higher Wind Conditions (5 m/s)

Air concentrations generated by PDM are generally lower than ACAS (Figure 4d). However, the values over the territory of Hong Kong differ by less than 250%. As stronger winds advance the plume at a faster rate, the duration that radioactive material stays in a grid cell will be reduced. Therefore, as shown in Table 3, the simulated air concentrations obtained with both models are smaller than those obtained with lighter winds.

3.1.2 Ground Deposition

Ground deposition is normally defined as the amount of radiation caused by the deposition of radioactive material on the ground surface. However, as explained in Appendix V, depletion of the radioactive material is used to represent the amount of ground deposition in PDM.

The simulated results for ground deposition from both models are shown in Table 4. They show that the values are comparable and that within the territory of Hong Kong, the difference in the simulated ground deposition between PDM and ACAS is generally within one order of magnitude.

(a) Light Wind Conditions (2 m/s)

Under very unstable atmospheric conditions, i.e. Category B, the results shown in Figure 5a indicate that both PDM and ACAS produce similar curves with almost the same slope, suggesting very similar dispersion characteristics between the models. The difference in ground deposition is less than 50%.

For neutral and very stable conditions, PDM produces a lower ground deposition especially at distances near the source than ACAS. Moreover, the slopes of the curves of

PDM are smaller than those of ACAS (Figures 5b-c). The difference in ground deposition between the models is within 4 times for Category D and F within the territory of Hong Kong.

(b) Higher Wind Conditions (5 m/s)

The simulation results are similar to light wind conditions for Category D, i.e. lower ground deposition and smaller slope. The difference in ground deposition between the two models is within one order of magnitude. Similar to air concentration, lower ground deposition is obtained under higher wind speed than under light wind conditions (Table 4).

3.1.3 External and Internal Doses

Besides air concentration and ground deposition, four other doses to the human body calculated by PDM and ACAS are also compared. They include the whole body dose, the thyroid dose, the lung dose and the skin dose. As discussed previously, dose conversion factors for internal and external doses are based on a study in Germany (Jacob *et al*., 1990) and the breathing rates are extracted from ICRP publication (1995).

Similar to air concentration and ground deposition, the dose values are 24-hour integrated dosage near the ground level. In the computation, thyroid dose and lung dose are associated solely with inhalation while whole body dose and skin dose include external exposure. No intervention measure is assumed in the calculations.

As doses are calculated based on simulated air concentration and ground deposition obtained from the models, comparison results of external and internal doses are similar to air concentration and ground deposition with modifications by the dose conversion factors.

3.1.3.1 Whole Body Dose

Whole body dose refers to the effective dose which is the sum of the weighted equivalent doses for all tissues and organs in a human body, and involves an internal and an external component.

Table 5 suggests that the whole body dose ranges from 10^{-11} to 10^{-13} mSv for region over Hong Kong under the designed release scenario. The simulation result shows that the slope of the whole body dose curves basically follows those obtained for air concentration and ground deposition (Figure 6).

The difference in dosage between the two models is within 7 times for Category B and D under light wind conditions (Figures 6a-b). However, with a less horizontally dispersed plume simulated by PDM in very stable atmosphere (i.e. Category F), the whole body dose at the centreline for PDM can be up to 35 times of those obtained from ACAS at 70 km downwind of GNPS (Figure 6c).

It may be worth noting that PDM generally tends to be more conservative in simulating whole body dose under low wind speeds. On the other hand, under neutral and well mixed conditions (i.e Category D under winds of 5 m/s), both PDM and ACAS simulated similar whole body doses downwind from the source (Figure 6d), with a difference of less than 60%.

3.1.3.2 Thyroid Dose

In case of a nuclear emergency, radioactive iodine could be released from the source along with other radionuclides. However, iodine is easily absorbed by thyroid in the human body. With a biological half-life of 8 days, the iodine can give the thyroid and nearby organs a high radiation dose through continuous internal exposure.

As only the early phase of an event is considered in the comparison exercise, the thyroid dose due to inhalation alone will be calculated. As in inhalation dose, thyroid dose is largely related to the radionuclide concentration in the air. Dosage from ingestion will be received at a much later stage and will not be considered here.

Table 6 shows that the 24-hour accumulated thyroid dose ranges from 10^{-9} to 10^{-11} mSv over Hong Kong with a 1 Bq/s release of I-131 for 3 hours. The comparison result is very similar to that for the whole body dose. PDM seems to be more conservative in simulating thyroid dose at distances of more than 20 kilometres away from the source under light wind conditions. For Category B, the thyroid dose calculated by PDM is about 3 to 4 times of those by ACAS (Figure 7a). For Category D, both PDM and ACAS perform similarly with a difference of within 300%. In contrast, the difference can be up to 16 times for Category F (i.e. very stable case) 70 km downwind from the source (Figure 7c). Both models, however, perform quite similarly under moderate wind conditions (Figure 7d) with a difference in thyroid dose of less than 250%.

3.1.3.3 Lung Dose

According to ICRP (1995), when performing dose calculations, the lung refers to the thoracic airways inside a human body that stretches from trachea through bronchi and bronchioles to the alveoli. Minute radioactive material can deposit along the thoracic airways and irradiate the body.

While iodine mostly affects the thyroid, the lung dose due to radioiodine exposure is comparatively small in amount. Table 7 shows that the lung dose only ranges from 10^{-12} to 10^{-14} mSv over Hong Kong with the designed release rate. It should be pointed out that in a real emergency situation, the organ is sensitive to some other elements such as thorium and therefore the lung dose due to these elements should not be neglected.

Results show that, same as for thyroid dose, the lung dose calculations by PDM are similar to those by ACAS. For light wind conditions, the lung dose of PDM is higher than that of ACAS at distances of more than 20 kilometres from the source. For Category B and D, the lung dose of PDM is at most 4 times of those calculated by ACAS (Figures 8a-b), with a larger discrepancy of about 15 times for Category F (i.e. very stable case) 70 km downwind from the source (Figure 8c). For moderate wind conditions, the difference between the two models is largest at distances near the source, amounting to 240%, but the discrepancy decreases for regions further downwind to about 40% at 70 kilometres downwind from the source (Figure 8d).

3.1.3.4 Skin Dose

Although a small amount of skin dose is related to inhalation, it is mainly caused by external exposure shine by plume or ground deposition in the early phase (ICRP, 1995).

Table 8 tabulates the skin dose caused by the exposure of I-131 as simulated by the two models under the designed scenario. It is observed that the skin dose is relatively small comparing to other doses and ranges from 10^{-11} to 10^{-15} mSv. It is noticed that PDM estimates a smaller dose than ACAS (Figures 9a-d). Under light wind conditions, results simulated by PDM are about one order of magnitude less than those by ACAS for Category B. The difference is up to about 30 times at a distance of 10 km downwind from the source for Category D (Figure 9b). This discrepancy widens up to 70 times for region close to the source under well mixed condition with moderate wind speed (Figure 9d).

The larger discrepancy in skin dose simulated by the two models may be a result of combined discrepancies caused by the external and internal dose terms. For the external doses, both the plume shine (air concentration) and the ground shine (ground deposition) of the plume could introduce discrepancies in the simulation. The discrepancies from the external dose would add to those contributed by the internal dose. All these discrepancies in the calculation tend to accumulate and the total differences could mount up to two orders of magnitude.

3.2 Cross-wind Spread

Besides comparing values along the centreline of a plume, the cross-wind plume spread is also investigated. As the plume shape is similar for all quantities, only the air concentration is plotted for comparison. The plume spread is analyzed by plotting air concentration against the angle from the centreline at various distances downwind from the release site, i.e. 15, 25, 35, 45.5, 55.5 and 70 km, under different atmospheric conditions i.e. 2 m/s winds for very unstable (Category B), neutral (Category D) and very stable (Category F) conditions, and at 5 m/s winds for neutral atmosphere (Category D) (Figures 10-13).

ACAS outputs simulated values at specific distances and directions downwind from the source, which are called spider grids. However, PDM only outputs in grid point format. For easy comparison, the values at grid points of PDM closest to the spider grids under consideration are used in the comparison.

Under light wind and very unstable conditions, i.e. Category B as well as moderate wind and neutral conditions i.e. category D, the plume spreads simulated by the two models are in general agreement. For Category B under light wind conditions, the plume width ranges about 15° on either side of the centreline, i.e. 30° for the whole plume. For Category D under moderate wind conditions, the whole plume spans about 20° to 25°.

For the very stable case, i.e. Category F under light wind conditions, the plume width simulated by PDM is in general less than 10° and is narrower than that of ACAS, which is more than 15°. It can be inferred from Figure 12 that the air concentration along the centreline simulated by PDM at distances close to the source is lower than ACAS. However, because of a narrower plume spread, the air concentration along the centreline becomes higher than ACAS at distances further downwind. The narrow plume spread of PDM may be a result of a more restricted horizontal dispersion of radioactive material than ACAS. Particles tend to concentrate near the centreline and disperse slowly outward while being transported downwind by the prevailing wind.

A narrower plume spread of PDM, though less obvious, can also be observed for Category D under light wind conditions especially at distances further away from the source.

4. Conclusion and Discussion

The Hong Kong Observatory has developed a PDM. It is a modular system consists of four modules, namely the Meteorological Module, the Dispersion Module, the Dose and Protective Action Module, and the Interface and Control Module.

The Meteorological Module ingests surface observations, numerical weather prediction model output, rainfall and radar data, and terrain information, through variational method, to produce the 3-dimensional wind fields, rainfall and stability fields. With these meteorological data, the Dispersion Module estimates the air concentration and ground deposition of the radioactive material using a random-walk particle model. The Dose and Protective Action Module then calculates the doses that the public would be exposed to. The module also estimates the reduced dose as a result of different protective actions, such as evacuation and sheltering. The Interface and Control Module includes user-friendly graphical user interfaces for submitting runs and outputting model results.

The results obtained by PDM were compared against those by ACAS for air concentration, ground deposition and various doses downwind along the centreline of the plume. Despite the fundamental differences in the handling of dispersion by the two models, the comparison results show that the discrepancies between the two models on various quantities are generally within one order of magnitude over the territory of Hong Kong. Moreover, the horizontal plume spreads simulated by both models are comparable under different atmospheric stabilities.

With these results, PDM can thus serve as an easily accessible and alternative reference to help users better understand the atmospheric and dispersion processes in the event of a radiological emergency.

ACKNOWLEDGEMENT

The authors would like to thank Dr. T. Yoshikawa of the Science University of Tokyo, Dr. Masamichi Chino and Dr. Akiko Furuno of the Japan Atomic Energy Research Institute for the exchange of experience on accident consequence assessment systems.

REFERENCES

1. Ahlstrom, S. W., H. P. Foote, R. C. Arnett, C. R. Cole, and R. J. Serne 1977 Multicomponent Mass Transport Model: Theory and Numerical Implementation (Discrete – Parcel – Random-Walk Version), BNWL-2127, Battelle, Pacific Northwest Lab., Richland, Washington, USA.

2. Brenk, H. D. and K. J. Vogt 1981 The Calculation of Wet Deposition from Radioactive Plumes, *Nuclear Safety*, **22**, No. 3, p. 362-371.

3. Cheng, C. M., C. M. Tam and E. Koo 1989 Determination of Atmospheric Stability by Turner's Method, Hong Kong Observatory Section Note No. 31 (Internal).

4. Eckerman K. F. and J .C. Ryman 1993 External Exposure to Radionuclides in Air, Water and Soil, Federal Guidance Report No. 12, EPA 402-R-93-081, Oak Ridge National Laboratory, Oak Ridge, Tennessee; US EPA, Washington DC, USA.

5. Etling, D., J. Preuss and M. Wamser 1986 Application of a Random Walk Model to Turbulent Diffusion in Complex Terrain, *Atmos. Environ.*, **20**, No. 4, p. 741-747.

6. Furuno, A., M. Chino, and H. Yamazawa 1999 Worldwide Version of System of Prediction of Environmental Emergency Dose Information (WSPEEDI) Model Code (II) – Three-dimensional Atmospheric Dispersion Model for Synoptic Scale: GEARN, JAERI-Data/Code 99-044, Japan Atomic Energy Research Institute, Japan.

7. International Commission on Radiological Protection 1995 Age-dependent Doses to Members of the Public from Intake of Radionuclides: Part 4 Inhalation Dose Coefficients, ICRP Publication 71, Pergamon Press, Oxford.

8. Imai, K., M. Chino, H. Ishikawa, M. Kai, K. Asai, T. Homma, A. Hidaka, Y. Nakamura, T. Iijima, and S. Moriuchi 1985 SPEEDI: A Computer Code System for the Real-Time Prediction of Radiation Dose to the Public due to an Accidental Release, JAERI 1297, Japan Atomic Energy Research Institute, Japan.

9. Jacob, P., H. Rosenbaum, N. Petoussi, M. Zankl 1990 Calculation of Organ Dose from Environmental Gamma Rays Using Human Phantoms and Monte Carlo Methods, GSF Bericht 12/90.

10. Lam, C. C. and H. Y. Yeung 2003 Impact of Radar Data on Model Forecast of Heavy Rain Associated with Landfalling Tropical Cyclone. Proceedings of International Workshop on NWP Models and Heavy Precipitation in Asia and Pacific Areas, Tokyo, Japan, p. 106-113.

11. Ley, A. J. 1982 A Random Walk Simulation of Two-dimensional Turbulent Diffusion in the Neutral Surface Layer, *Atmos. Environ.*, **16**, No. 12, p. 2799-2808.

12.	Li, P. W., W. K. Wong, K. Y. Chan and Edwin S. T. Lai	2000	SWIRLS – An Evolving Nowcasting System, Hong Kong Observatory Technical Note No. 100.
13.	Neal, A. P. and M. C. Davies	1987	Consultancy on the Environmental Aspects of the Daya Bay Nuclear Power Station for the Government of Hong Kong: Contingency Planning, Government Printer, Hong Kong.
14.	Ove Arup / Electrowatt	1993	Study on Shielding Effectiveness of Building in Hong Kong, Executive Summary Report. Consultancy Agreement No.DHCR/MISC/254(D).
15.	Pasquill, F. and F. B. Smith	1983	Atmospheric Diffusion, 3rd Edition, Ellis Horwood Limited, pp. 437.
16.	PLG	1991	Design Description for the Radiological Accident Consequence Assessment System (ACAS).
17.	Ross, D. G. and D. G. Fox	1991	Evaluation of an Air Pollution Analysis System for Complex Terrain. *J. Appl. Meteor.*, **30**, p. 909-923.
18.	Ross, D. G., I. N. Smith, P. C. Manins and D. G. Fox	1988	Diagnostic Wind Field Modelling for Complex Terrain: Model Development and Testing. *J. Appl. Meteor.*, **27**, p.785-796.
19.	Sehmel, G. A.	1980	Particle and Gas Dry Deposition: A Review, *Atmos. Environ.*, **14**, p. 983-1011.
20.	Sherman, C. A.	1978	A Mass-consistent Model for Wind Fields over Complex Terrain. *J. Appl. Meteor.*, **17**, p. 312-319.
21.	Slade, D. H.	1968	Meteorology and Atomic Energy – 1968, USAEC Report TID-24190, Air Resources Laboratory, NTIS.
22.	Thomson, D. J.	1986	A Random Walk Model of Dispersion in Turbulent Flows and its Application to Dispersion in a Valley, *Quart. J. R. Met. Soc.*, **112**, p. 511-530.
23.	Tian, G. and X. Y. Wang (田鋼及王醒宇)	2001	Offsite Nuclear Accident Consequence Forecast and Assessment System in Guangdong Nuclear Power Station, Radiation Protection, **21**, no. 4, p. 208-218. (in Chinese)
24.	Venkatesan, R., Möllmann-Coers M. and Natarajan A.	1997	Modeling Wind Field and Pollution Transport over a Complex Terrain Using an Emergency Dose Information Code SPEEDI, *J. Appl. Meteor.*, **36**, p. 1138-1159.
25.	Yoshikawa, T.	2001	Personal communication.
26.	Zannetti, P.	1990	Air Pollution Modelling: Theories, Computational Methods and Available Software, Computational Mechanics Publication, pp. 444.

APPENDIX I

Variational method used in PDM

The fundamental difference between PDM and ACAS is that the former employs 3-dimensional wind fields for estimating dispersion. The variational method was first applied by Sherman (1978) to dispersion models for the simulation of 3-dimensional wind field. In essence, the method seeks to minimize an integral function which represents the difference between the initial wind field and the final wind field by iteration, subject to the constraint that the divergence should vanish, i.e. mass conservation (Ross *et al.*, 1988):

$$E = \int \alpha_1^{\,2}(u-u_0)^2 + \alpha_1^{\,2}(v-v_0)^2 + \alpha_2^{\,2}(w-w_0)^2 + \lambda\left[\frac{\partial u}{\partial x} + \frac{\partial v}{\partial y} + \frac{\partial w}{\partial z}\right] dV$$

where u_o, v_o, w_o – x, y, and z components of the initial winds at each grid point (m/s)

u, v, w – the corresponding adjusted wind components after analysis by variational method (m/s)

α_1, α_2 – weighting of the horizontal and vertical wind components respectively

λ – Lagrangian multiplier

The first three terms on the right-hand side represent variation of the three wind components. The fourth term implements the constraint of mass conservation or non-divergence in the minimization process. The parameters α_1 and α_2, commonly called the Gauss Precision Moduli, incorporate the thermodynamic effect in the variational method. The ratio α_1/α_2 prescribes the fraction of adjustment to be made to the horizontal and vertical wind components. When the ratio is small, the horizontal adjustment dominates and the airflow goes around topographical obstacles, i.e. the atmosphere is stable. When the ratio is large, the flow goes over the obstacles, i.e. the atmosphere is unstable. In the System for Prediction of Environmental Emergency Dose Information (SPEEDI) of Japan Atomic Energy Research Institute (JAERI) (Imai *et al.*, 1985), the ratio was taken to be constant throughout the whole domain. Some literature (Venkatesan *et al.*, 1997) described ways to include variation of the moduli in the vertical direction. For PDM, α_1 is assigned a value of 1, while α_2 is assigned values of 5, 10, 15, 20, 30, 50, and 70 for the stability Categories A to G respectively (Yoshikawa, 2001).

APPENDIX II

Domain size, grid setting and terrain information

A. Domain Size and Grid Setting

To incorporate terrain forcing over Hong Kong and its vicinity, PDM employs a terrain-following coordinate system with variable vertical grid spacing. The horizontal domain covers a total area of 160 km x 160 km with Hong Kong at the centre and Daya Bay to the northeast (Figure II-1). The vertical grid consists of 20 layers. The lowest layer is adjacent to the ground surface while the model top reaches a height of 1440 m, matching the surface and approximately the 850 hPa level of ORSM respectively. This setting is adequate for modeling short range dispersion as most atmospheric processes related to this take place within the planetary boundary layer which is normally below 850 hPa. The height of the K^{th} layer (K=1, 2, … ,20) at horizontal grid point (I,J) is defined by the following equation:

$$ZS(I,J,K) = T(I,J) + Z(K) * \frac{(ZT - T(I,J))}{ZT}$$

where *ZS(I,J,K)* – height of the K^{th} layer at horizontal grid (I,J)

T(I,J) – terrain height at horizontal grid (I,J)

Z(K) – height of the K^{th} layer for flat terrain

ZT – height of the top layer, i.e. 1440 metres (roughly the height of 850 hPa level)

B. Terrain Information

Unlike ACAS, PDM takes account of terrain effect when simulating the 3-dimensional wind field. The global 1-km resolution topography file prepared by the United States Geological Survey (USGS) is used to represent terrain heights for the entire domain. Each grid cell covers an area of 1 km x 1 km. The elevation data are important in calculating the vertical component of the wind speed using the variational method. Figure II-2 shows a 3-dimensional plot of terrain height over the simulation domain.

APPENDIX III

Random-walk particle approach

The random-walk particle dispersion model used in PDM follows the stochastic approach (also called Monte Carlo approach) and employs a certain number of fictitious particles to simulate the kinematics of the radioactive material released. Radioactivity is apportioned evenly to each fictitious particle according to the source term. Particle motion is produced by semi-random pseudo-velocities generated using the Monte Carlo technique. Important characteristics of the dispersion process can be inferred from the average particle ensemble properties, which are not affected by the randomness of the velocity if a sufficient number of particles are used (Zanetti, 1990). Air concentration and ground deposition are calculated based on the assigned radioactivity after correction for decay.

The movement or the location of each fictitious particle can be estimated by the following expressions (Ahlstrom *et al*., 1977; Furuno *et al*., 1999):

$$x_i(t+\Delta t) = x_i(t) + u_i \Delta t + R_x$$

$$y_i(t+\Delta t) = y_i(t) + v_i \Delta t + R_y$$

$$z_i(t+\Delta t) = z_i(t) + w_i \Delta t + R_z$$

$$R_x = \sqrt{2K_x \Delta t}S \qquad R_y = \sqrt{2K_y \Delta t}S \qquad R_z = \sqrt{2K_z \Delta t}S$$

where	x_i, y_i, z_i	–	location of particle i
	$u_i\Delta t, v_i\Delta t, w_i\Delta t$	–	transport term
	R_x, R_y, R_z	–	dispersion term
	K	–	dispersion coefficient (m^2/s)
	S	–	random number (mean = 0; standard deviation = 1)

The dispersion coefficient, K, is a function of wind velocity (Ahlstrom *et al*, 1977). This quantity can be estimated by a set of analytical equations under different atmospheric stability categories. In PDM, the formulae developed for the urban areas by Brigg (Pasquill and Smith, 1983) are used for the computations. These formulae are listed in Appendix VIII.

Considering the stochastic nature of the model, the exact positions of individual particle are meaningless. The individual positions have to be viewed collectively to give an ensemble distribution for the plume. In the process, a grid system is required as the position reference so that the distribution of the particles at a certain time is computed by counting the number of particles within each grid cell (Zanetti, 1990).

To apply PDM to the dispersion of radioactive material, an amount of radioactivity, according to the source term, is apportioned evenly to each particle at the start of the simulation.

The instantaneous air concentration at each grid is the sum of each particle's activity within that grid at a certain time, whereas the ground deposition is the sum of those "deposited" onto the ground. The time integrated air concentration and ground deposition are accumulated in each time step.

APPENDIX IV

Radioactive Decay

The radioactive decay process is simulated by an exponential decrease of the activity assigned to each particle. According to the type of radionuclides, the radioactivity for each particle is obtained by multipling by the exponential function in each time step.

$$q = q_0 * \exp(D * \Delta t)$$

where	q_0	–	original activity of the particle (Bq)
	q_0	–	new activity of the particle (Bq)
	D	–	decay constant of the radionuclide (s^{-1})
	Δt	–	duration of time step, i.e. 60 seconds

PDM accepts as many as 8 different types of radionuclides for the radioactivity decay calculation. The total radioactivity is obtained by summing the contributions from all the radionuclides.

APPENDIX V

Estimation of dry and wet depositions

A. Dry Deposition

Dry deposition is treated in a special manner in PDM. As the Monte Carlo method is used, the number of fictitious particles has to be large enough to enable an accurate description of the plume shape. In order to preserve the number of particles, landed particles are treated as temporary depletion of radioactivity instead of physically deposited on ground permanently. That means the particles can later be transported and dispersed in the atmosphere again. Deposition is counted only when the particle is located within the lowest layer in the model. Owing to the rugged terrain in Hong Kong, the model treats the particles as on the terrain surface if they move below the terrain height.

The removal of radioactive matter from the atmosphere due to dry deposition is calculated by the expressions (Furuno *et al*., 1999) below:

$$\frac{dq_n}{dt} = -kv_g q_n$$

$$k = \frac{2}{\Delta z}(1 - \frac{z_p}{\Delta z})$$

where q_n – radioactivity of the particle n (Bq)

v_g – deposition velocity of a specific radionuclide (m/s)

z_p – height of particle above ground (m)

Δz – depth of the lowest layer (m), where $z_p < \Delta z$

For radioactivity in gaseous form, dry deposition is strongly affected by its chemical interaction with ground surface (Zanetti, 1990). Sehmel (1980) pointed that the deposition velocity varies substantially for each species. Its range covers three orders of magnitude, from 0.02 to 26 cm/s for iodine. Noble gases, however, have no chemical reaction with the surface and thus their deposition velocities are negligible.

C. Wet Deposition

Wet deposition of radioactive material, or tropospheric particles in general, is primarily accomplished by two mechanisms, namely ‘rainout’ and ‘washout’ (Slade, 1968).

Rainout is the process of particles becoming entrained into cloud droplets, either by nucleation or by scavenging, and are subsequently removed from the atmosphere along with cloud water during precipitation. Washout is particle scavenging by falling precipitation. The scavenging process of washout consists of repeated exposures of particles and gases to cloud or precipitation elements with some chance of accretion by the elements for each exposure. For the purpose of dose assessment in the case of reactor accident, wet deposition is regarded as the depletion of radioactivity due to precipitation. This depletion can be estimated using an exponential decay process obeying the equation (Brenk and Vogt, 1981) below:

$$\frac{dq_n}{dt} = -\Lambda q_n \qquad (\Lambda = \alpha\gamma^{\beta})$$

where	q_n	–	radioactivity of the particle *n* (Bq)
	Λ	–	washout rate, which is a function of rainfall rate
	α,β	–	factors dependent upon the type of radionuclides (Appendix VIII)
	γ	–	rainfall rate (mm/hr)

In PDM, rainfall information is extracted from the Observatory's Short-range Warning of Intense Rainstorms in Localized Systems (SWIRLS) (Li *et al.*, 2000) and ORSM to generate grid-point values of hourly rainfall. Hourly rainfall analyses from SWIRLS, derived from radar reflectivity and calibrated by surface rain-gauge observations, are averaged over 5 km x 5 km horizontal grids. Rainfall prediction from ORSM is Cressman interpolated to provide forecast hourly rainfall in grids.

APPENDIX VI

Dose Coefficients and Estimation of External and Internal Doses

A. Dose Coefficients

From the estimated air concentrations and deposition density, the dose to the various body organs and whole body arising from the different exposure pathways can be computed. In PDM, the population is divided into three age groups: infant (age 1), child (age > 1 and < 17) and adult (age 17 or above) (ICRP, 1995). In general, the inhalation dose is quite age dependent with children being the most sensitive group. There is normally very little age dependency in terms of external irradiation.

Dose calculations are performed using dose conversion factors (DCF). The dose resulting from exposure to the air concentration or ground deposition of a particular nuclide ***i*** through a particular pathway ***j*** may be expressed as:

$$Dose_{i,j} = X_i * (DCF)_{i,j}$$

where X_i is the air concentration or deposition density of nuclide ***i***.

Age-dependent DCFs for members of the public are based on a study in Germany (Jacob *et al.*, 1990). For inhalation, DCFs are for acute intake, which is suitable for estimating dose during the early phase of release of radioactive material. The values of DCF for different radionuclides of various age groups for both external and internal doses are tabulated in the Appendix VIII.

B. External Dose

Two exposure modes are included in the estimation of external dose. They are:

i. immersion in a contaminated plume (plume shine); and
ii. exposure to a contaminated ground surface (ground shine).

The DCFs for external exposure used in this model are provided by JAERI based on a study in Germany (Jacob *et al.*, 1990) to calculate the external exposure due to plume shine by the radionuclides in the air and ground shine by those deposited on the ground surface (shown in the Appendix VIII).

Estimation of doses to the tissues of a body from radiation due to an arbitrary distribution of a radionuclide in an environmental medium is an extremely difficult computational task. The common practice is to consider simplified and idealized exposure geometries, i.e. the radionuclide concentration in the medium, seen from the location of an exposed individual near the ground surface, is assumed uniform and effectively infinite or semi-infinite in extent. In Eckerman and Ryman (1993), for example, a semi-infinite source region is assumed for submersion in a radioactive plume and an infinite source region is assumed for exposures to ground contamination. In PDM, the above assumptions are followed and the "effective" air concentrations are assumed to be the concentrations at the lowest layer.

The external dose received by the human body for each time step can be calculated by the following expression for a specific radionuclide:

$$D_{ext} = (F_{ext,air} C_{ij1} + F_{ext,gd} C_{gd,ij})(\frac{\Delta t}{3600})$$

where	D_{ext}	–	external dose (mSv)
	$F_{ext,air}$	–	the DCF for external plume shine of different age group [(mSv/h)/(Bq/m^3)]
	$F_{ext,gd}$	–	DCF for external ground shine of different age group [(mSv/h)/(Bq/m^2)]
	C_{ij1}	–	air concentration at grid I,J of level 1, i.e. near surface (Bq/m^3)
	$C_{gd,ij}$	–	ground deposition at I,J (Bq/m^2)
	Δt	–	duration of time step, i.e. 60 seconds

C. Internal Dose

Besides external exposure, another major exposure pathway during the early phase of radioactive release is through inhalation. Only the inhalation of radioactive particulates in the plume is considered in this model. Doses due to inhalation of re-suspended particulates are not included in view of its small contribution to the total dose.

Radioactive material inhaled into the human body will deposit onto and be absorbed by the respiratory tract. Some of the radioactive material will be cleared by the body metabolic process while the remainder will stay in the body for the whole life. Thus the time-integrated total doses (committed equivalent and effective doses) depend on the age at which the radioactive material is inhaled.

In this model, the public is categorized into three age groups according to age ranges defined by the ICRP (1995):

Infant: from 0 to 12 months old
Child: from 1 to 17 years old
Adult: older than 17 years

The "child" group covers four age ranges, namely one year, five years, 10 years and 15 years. To be conservative, dose coefficients and the corresponding breathing rates (to be discussed shortly) of the age range that give rise to the highest whole body doses are used in the model for different radionuclides, i.e. those of age one year for I-131 and age 15 years for Cs-137 and Sr-90.

Age-dependent dose coefficients for members of the public for intakes by inhalation of radioisotopes are extracted from ICRP publication (1995). The dose coefficients are for acute intake, which suits the purpose of estimating dose during the early phase of release of radioactive material. The integration times for the committed doses are assumed to be 50 years for adult and from time of intake to age 70 years for infant and child.

Noble gases are insoluble and non-reactive with negligible deposition in the respiratory tract (ICRP, 1995). Thus no dose coefficient is assigned to noble gases as no contribution to the dose is expected from them through the inhalation pathway.

Uptake by body fluids of dissociated radioactive material after being inhaled is broadly categorized into Type F (fast), M (moderate) and S (slow) in ICRP publication (1995). Dose coefficients of the default type recommended by ICRP (1995) for each individual radionuclide are extracted. As for radioiodine, absorption also depends on its physical (e.g. particulates) and chemical forms (e.g. methyl iodide). In the absence of information on its form in the radioactive plume, the dose coefficients of the form of radioiodine that results in the most whole body dose, i.e. elemental form, is chosen on conservative consideration.

Another factor that affects the amount of radioactive material inhaled is the breathing rates (m^3/h), which depend on age, body size and level of physical activity. ICRP (1995) provides daily time budget and ventilation parameters at each exercise level for members of the public at various ages. Based on the figures, the daily average breathing rate for infant, child and adult are calculated and used in the model. For child group, those of the age ranges are chosen as discussed in the early part of this Appendix. The breathing rates are listed in the Appendix VIII.

The internal dose received by each organ can be calculated using the following expression for each time step.

$$D_{inh} = F_{inh} B C_{ij1} \left(\frac{\Delta t}{3600}\right)$$

where D_{inh} – internal dose for each organ (mSv)

F_{inh} – inhalation dose coefficient for each organ of different age group (mSv/Bq)

B – breathing rate (m^3/h)

C_{ij1} – air concentration at grid I,J of level 1, i.e. near surface (Bq/m^3)

Δt – duration of time step, i.e. 60 seconds

APPENDIX VII

Protective Actions in the Event of a Nuclear Power Station Accident

For an off-site or potential off-site accident, protective actions, including sheltering, evacuation and relocation, may be initiated with a view to reducing the dose to the public. In the DBCP, protective actions are considered in order to reduce the doses due to external exposure and inhalation of radioactive material from the plume.

Plume countermeasures, if necessary, are implemented during the early phase of radioactive releases, targeted at the external exposure and inhalation pathways. Among the plume countermeasures, dose reduction due to evacuation and sheltering are estimated by this model. For evacuation, the dose increment at a certain location is simply set to zero once the people are evacuated. Thus the total dose to these people is that up to the point of evacuation.

As for sheltering, the amount of dose reduced is characterized by the shielding factor of the shelter, which is defined, in general terms, as the ratio of the dose rate that a person would receive within a building to that which he would receive in the open air (Ove Arup/Electrowatt, 1993). A shielding factor of 0.1 for building means a reduction of 90% in the dose rate when an individual is inside that building comparing to being in the open air.

The shielding factors depend strongly on the type of building that the public take shelter. According to the study by Ove Arup/Electrowatt, the shielding factor for plume shine ranged from 0.007 for villa/modern village housing to 0.3 for temporary housing/squatter huts. The shielding factors for ground deposition ranged from 0.024 for solid wall construction offices to 0.5 for temporary housing/squatter huts. As most people in Hong Kong spend a major portion of their time in their homes which are mainly public housing or private house flats, the shielding factors of these housing or flats are chosen for the dose model. The shielding factor for inhalation as a result of sheltering indoors is given by Neal and Davies (1987) assuming that air exchange between indoor and outside is restricted. The shielding factors are shown in the Appendix VIII.

APPENDIX VIII

Numerical Parameters Used in PDM

Estimates of the Pasquill-Gifford σ_y and σ_z formulae by Brigg for elevated small releases as a function of downwind distance x (Pasquill and Smith, 1983)

Stability Category	σ_y	σ_z
A	$0.32\ x\ (1+0.4x)^{-0.5}$	$0.24\ x\ (1+0.1x)^{0.5}$
B	$0.32\ x\ (1+0.4x)^{-0.5}$	$0.24\ x\ (1+0.1x)^{0.5}$
C	$0.22\ x\ (1+0.4x)^{-0.5}$	$0.20\ x$
D	$0.16\ x\ (1+0.4x)^{-0.5}$	$0.14\ x\ (1+0.3x)^{-0.5}$
E	$0.11\ x\ (1+0.4x)^{-0.5}$	$0.08\ x\ (1+0.15x)^{-0.5}$
F	$0.11\ x\ (1+0.4x)^{-0.5}$	$0.08\ x\ (1+0.15x)^{-0.5}$

Decay coefficients of various radionuclides (Jacob *et al.*, 1999)

Decay Coefficient (s^{-1})	*I-131*	*I-132*	*I-133*	*Cs-134*	*Cs-137*	*Sr-90*	*Xe-133*
	9.98E-07	8.37E-05	9.26E-06	1.07E-10	7.33E-10	7.55E-10	1.53E-06

Factors for the calculation of washout rate of elemental iodine vapor and aerosols (Brenk and Vogt, 1981)

	Washout Rate [s^{-1}] [$\Lambda = \alpha\ \gamma^{\beta}$; γ = rainfall rate (mm/hr)]	
Particles	α	β
Elemental Iodine Vapor	8×10^{-5}	0.6
Aerosols	1.2×10^{-4}	0.5

Breathing rate of different age groups (ICRP, 1995)

	Breathing Rate [m^3/h]		
	Adult	*Child*	*Infant*
All radionuclides	0.12	0.84	0.93

Shielding factors for plume shine, ground shine, and inhalation (Ove Arup/Electrowatt, 1993)

	Shielding Factor		
	Plume Shine	*Ground Shine*	*Inhalation*
All radionuclides	0.048	0.1	0.1

APPENDIX VIII (continued)

Numerical Parameters Used in PDM

Dose conversion factors for external and internal exposures (Jacob *et al*., 1999)

Dose Conversion Factors for External Exposure						
	Plume Shine [(mSv/h)(Bq/m^3)]			Ground Shine [(mSv/h)(Bq/m^2)]		
	Adult	*Child*	*Infant*	*Adult*	*Child*	*Infant*
I-131	6.00E-08	6.70E-08	7.60E-08	8.90E-10	9.80E-10	1.20E-09
I-132	3.70E-07	4.20E-07	4.60E-07	5.10E-09	5.70E-09	6.80E-09
I-133	9.80E-08	1.10E-07	1.20E-07	1.40E-09	1.50E-09	1.90E-09
Cs-134	2.60E-07	2.90E-07	3.20E-07	3.60E-09	4.00E-09	4.80E-09
Cs-137	9.80E-08	1.10E-07	1.20E-07	1.40E-09	1.50E-09	1.90E-09
Sr-90	0	0	0	0	0	0
Xe-133	4.60E-09	5.20E-09	6.80E-09	0	0	0
Dose Conversion Factors for Internal Exposure						
	Whole Body Dose [mSv/Bq]			Thyroid Dose [mSv/Bq]		
	Adult	*Child*	*Infant*	*Adult*	*Child*	*Infant*
I-131	2.0E-08	9.4E-08	1.7E-07	3.9E-07	1.9E-06	3.3E-06
I-132	3.1E-10	1.3E-09	2.8E-09	3.6E-09	2.0E-08	4.3E-08
I-133	4.0E-09	2.1E-08	4.5E-08	7.6E-08	4.2E-07	8.9E-07
Cs-134	2.0E-08	4.1E-08	7.0E-08	4.3E-09	1.1E-08	1.7E-08
Cs-137	3.9E-08	7.0E-08	1.1E-07	3.6E-09	7.3E-09	1.1E-08
Sr-90	1.6E-07	2.7E-07	4.2E-07	3.4E-11	7.7E-11	2.3E-10
Xe-133	0	0	0	0	0	0
	Lung Dose [mSv/Bq]			Skin Dose [mSv/Bq]		
	Adult	*Child*	*Infant*	*Adult*	*Child*	*Infant*
I-131	6.9E-10	1.4E-09	2.7E-09	6.4E-11	1.7E-10	4.4E-10
I-132	6.0E-10	1.1E-09	2.2E-09	1.9E-11	5.7E-11	1.6E-10
I-133	6.5E-10	1.3E-09	2.5E-09	3.5E-11	1.1E-10	3.3E-10
Cs-134	1.4E-07	2.7E-07	4.5E-07	2.9E-09	5.1E-09	8.4E-09
Cs-137	3.0E-07	5.2E-07	8.2E-07	2.0E-09	3.5E-09	5.3E-09
Sr-90	1.3E-06	2.2E-06	3.4E-06	3.4E-11	7.7E-11	2.3E-10
Xe-133	0	0	0	0	0	0

TABLES

Stability Category	A	B	C	D	E	F	G
Percentage	1.0%	6.9%	12.2%	54.1%	13.1%	10.4%	2.3%

Table 1 Statistics of hourly stability categories at HKIA in 2003

<table>
<tr><th colspan="4">Input</th></tr>
<tr><td colspan="2">Source Location</td><td colspan="2">GNPS (25°35.8’N, 114°32.5’E)</td></tr>
<tr><td colspan="2">Radionuclides</td><td colspan="2">Iodine-131</td></tr>
<tr><td colspan="2">Release Rate</td><td colspan="2">1 Bq/s for 3 hours</td></tr>
<tr><td colspan="2">Release Height</td><td colspan="2">10 metres above surface</td></tr>
<tr><td colspan="2">Winds</td><td colspan="2">Northeasterly winds from 045° at 2 m/s and 5 m/s</td></tr>
<tr><td colspan="2">Stability</td><td colspan="2">Categories A to G</td></tr>
<tr><td>Rainfall</td><td>Nil</td><td>Terrain Effect</td><td>Flat terrain</td></tr>
<tr><td>Age Group</td><td>Adult</td><td>Protective Actions</td><td>Nil</td></tr>
<tr><th colspan="4">Output</th></tr>
<tr><td colspan="4">24-hour integrated amount along the centreline of the plume
and the cross-wind spread* of the following quantities</td></tr>
<tr><td colspan="2">Air concentration</td><td colspan="2">Ground deposition</td></tr>
<tr><td colspan="2">Whole body dose</td><td colspan="2">Thyroid dose</td></tr>
<tr><td colspan="2">Lung dose</td><td colspan="2">Skin dose</td></tr>
</table>

* At 15, 25, 35, 45.5, 55.5 and 70 km downwind from the source

Table 2 Input and output of the comparison between ACAS and PDM

Distance from source / Model	15 km	25 km	35 km	45.5 km	55.5 km	70 km	Stab. Cat.	Wind Speed
ACAS	1.9E-07	9.7E-08	7.2E-08	5.6E-08	4.4E-08	3.3E-08	B	2 m/s
PDM	5.4E-07	3.2E-07	2.3E-07	2.0E-07	1.5E-07	1.2E-07		
ACAS	1.8E-06	6.1E-07	3.3E-07	2.0E-07	1.4E-07	8.1E-08	D	
PDM	1.3E-06	7.4E-07	5.1E-07	4.1E-07	3.1E-07	2.2E-07		
ACAS	5.3E-06	1.3E-06	5.0E-07	2.1E-07	1.1E-07	3.9E-08	F	
PDM	4.3E-06	2.3E-06	1.6E-06	1.1E-06	9.0E-07	6.0E-07		
ACAS	9.4E-07	4.4E-07	2.6E-07	1.6E-07	1.1E-07	7.2E-08	D	5 m/s
PDM	2.9E-07	1.9E-07	1.3E-07	1.1E-07	7.8E-08	5.7E-08		

Table 3 24-hour integrated air concentration downwind along the plume centreline (Bq/m^3)

Distance from source / Model	15 km	25 km	35 km	45.5 km	55.5 km	70 km	Stab. Cat.	Wind Speed
ACAS	6.6E-06	3.3E-06	2.4E-06	1.8E-06	1.5E-06	1.2E-06	B	2 m/s
PDM	6.5E-06	3.4E-06	2.6E-06	2.1E-06	1.5E-06	1.3E-06		
ACAS	6.1E-05	2.1E-05	1.2E-05	6.8E-06	4.7E-06	2.8E-06	D	
PDM	1.5E-05	8.1E-06	5.5E-06	4.3E-06	3.3E-06	2.4E-06		
ACAS	1.9E-04	4.4E-05	1.8E-05	7.2E-06	3.7E-06	1.4E-06	F	
PDM	4.6E-05	2.5E-05	1.7E-05	1.2E-05	1.0E-05	6.6E-06		
ACAS	3.1E-05	1.5E-05	8.6E-06	5.3E-06	3.9E-06	2.6E-06	D	5 m/s
PDM	3.1E-06	1.9E-06	1.2E-06	1.1E-06	8.6E-07	5.6E-07		

Table 4 24-hour integrated ground deposition downwind along the plume centreline (Bq/m^2)

Distance from source / Model	15 km	25 km	35 km	45.5 km	55.5 km	70 km	Stab. Cat.	Wind Speed
ACAS	1.7E-12	8.7E-13	6.3E-13	4.7E-13	3.9E-13	2.9E-13	B	2 m/s
PDM	1.1E-11	5.9E-12	4.3E-12	3.8E-12	2.8E-12	2.2E-12		
ACAS	1.6E-11	5.5E-12	3.0E-12	1.7E-12	1.2E-12	6.9E-13	D	
PDM	2.4E-11	1.4E-11	9.5E-12	7.6E-12	5.7E-12	4.1E-12		
ACAS	4.8E-11	1.1E-12	4.5E-12	1.8E-12	9.2E-13	3.3E-13	F	
PDM	7.9E-11	4.3E-11	3.0E-11	2.1E-11	1.7E-11	1.1E-11		
ACAS	8.4E-12	3.9E-12	2.3E-12	1.4E-12	1.0E-12	6.9E-13	D	5 m/s
PDM	5.3E-12	3.5E-12	2.3E-12	2.0E-12	1.4E-12	1.1E-12		

Table 5 24-hour integrated whole body dose downwind along the plume centreline (mSv)

Model \ Distance from source	15 km	25 km	35 km	45.5 km	55.5 km	70 km	Stab. Cat.	Wind Speed
ACAS	6.8E-11	3.4E-11	2.5E-11	1.9E-11	1.6E-11	1.2E-11	B	2 m/s
PDM	2.0E-10	1.1E-10	8.3E-11	7.3E-11	5.4E-11	4.3E-11		
ACAS	6.3E-10	2.2E-10	1.2E-10	7.0E-11	4.8E-11	2.8E-11	D	
PDM	4.7E-10	2.7E-10	1.9E-10	1.5E-10	1.1E-10	8.0E-11		
ACAS	1.9E-09	4.5E-10	1.8E-10	7.3E-11	3.7E-11	1.3E-11	F	
PDM	1.5E-09	8.4E-10	5.8E-10	4.1E-10	3.2E-10	2.2E-10		
ACAS	3.3E-10	1.5E-10	9.0E-11	5.5E-11	4.0E-11	2.7E-11	D	5 m/s
PDM	1.0E-10	6.8E-11	4.5E-11	3.8E-11	2.8E-11	2.1E-11		

Table 6 24-hour integrated thyroid dose downwind along the plume centreline (mSv)

Model \ Distance from source	15 km	25 km	35 km	45.5 km	55.5 km	70 km	Stab. Cat.	Wind Speed
ACAS	1.3E-13	6.4E-14	4.7E-14	3.5E-14	2.9E-14	5.4E-14	B	2 m/s
PDM	3.5E-13	2.0E-13	1.5E-13	1.3E-13	9.6E-14	7.7E-14		
ACAS	1.2E-12	4.1E-13	2.2E-13	1.3E-13	8.9E-14	5.3E-14	D	
PDM	8.4E-13	4.7E-13	3.3E-13	2.6E-13	2.0E-13	1.4E-13		
ACAS	3.5E-12	8.3E-13	3.3E-13	1.4E-13	6.9E-14	2.5E-14	F	
PDM	2.7E-12	1.5E-12	1.0E-12	7.3E-13	5.7E-13	3.8E-13		
ACAS	6.1E-13	2.8E-13	1.7E-13	1.0E-13	7.5E-14	5.1E-14	D	5 m/s
PDM	1.8E-13	1.2E-13	7.9E-14	6.7E-14	5.0E-14	3.7E-14		

Table 7 24-hour integrated lung dose downwind along the plume centreline (mSv)

Model \ Distance from source	15 km	25 km	35 km	45.5 km	55.5 km	70 km	Stab. Cat.	Wind Speed
ACAS	4.8E-13	2.2E-13	1.5E-13	1.1E-13	8.2E-14	5.4E-14	B	2 m/s
PDM	6.5E-14	3.8E-14	2.8E-14	2.4E-14	1.8E-14	1.4E-14		
ACAS	4.4E-12	1.4E-12	7.3E-13	4.0E-13	2.5E-13	1.3E-13	D	
PDM	1.6E-13	8.8E-14	6.1E-14	4.9E-14	3.7E-14	2.7E-14		
ACAS	1.3E-11	3.0E-12	1.1E-12	4.2E-13	2.0E-13	6.3E-14	F	
PDM	5.1E-13	2.8E-13	1.9E-13	1.4E-13	1.1E-13	7.1E-14		
ACAS	2.4E-12	1.1E-12	6.3E-13	3.7E-13	2.7E-13	1.8E-13	D	5 m/s
PDM	3.4E-14	2.2E-14	1.5E-14	1.3E-14	9.3E-15	6.8E-15		

Table 8 24-hour integrated skin dose downwind along the plume centreline (mSv)

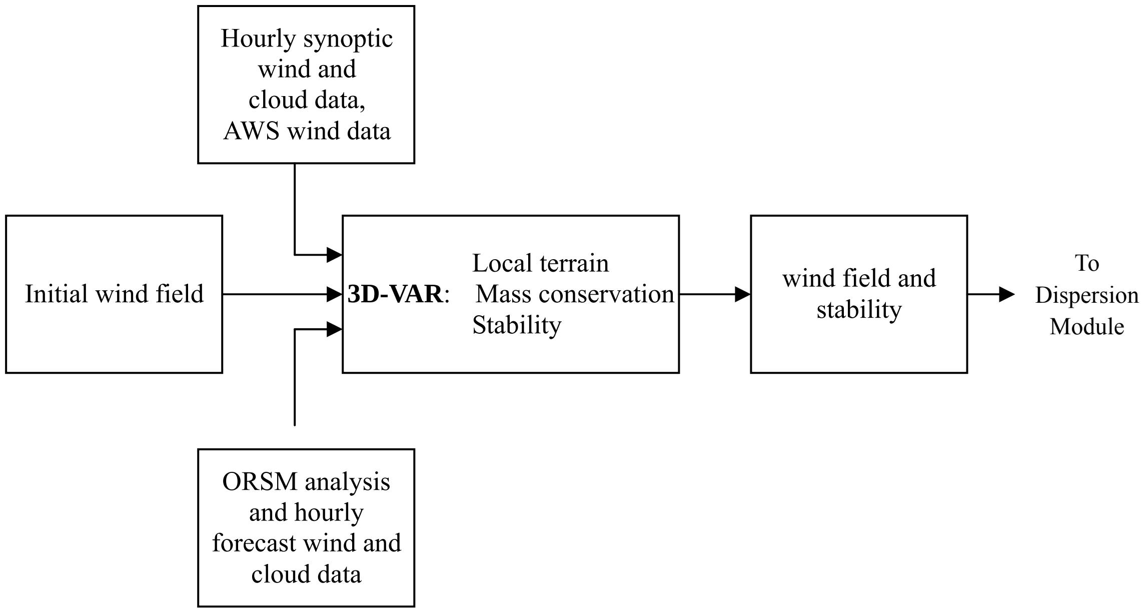

Figure 1 Block diagram of the Meteorological Module of PDM

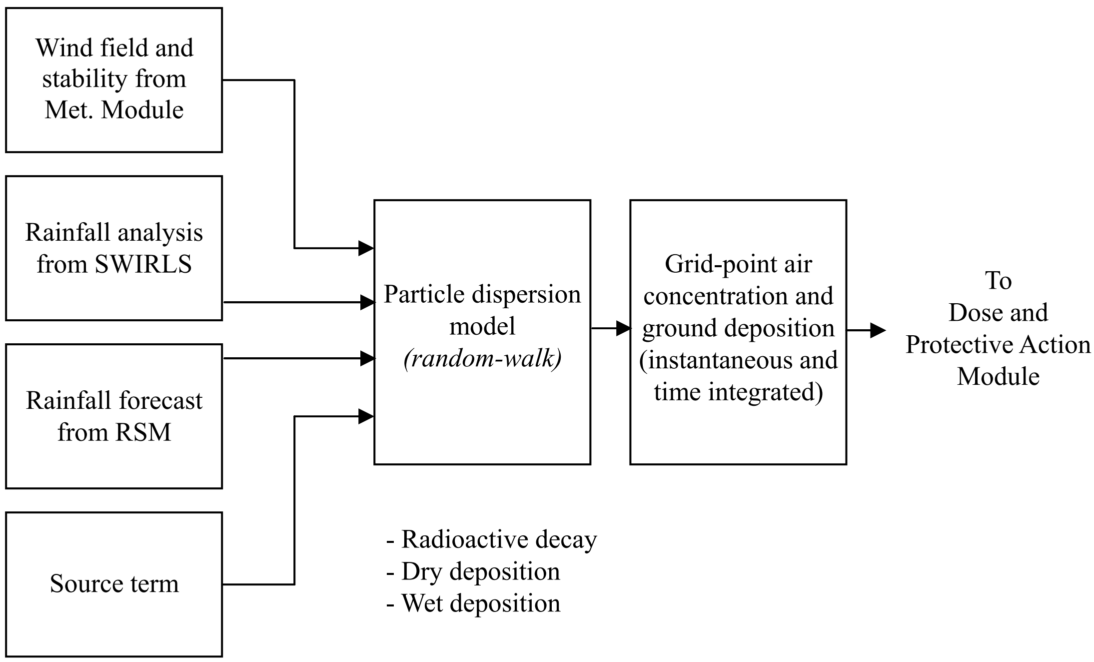

Figure 2 Block diagram of the Dispersion Module of PDM

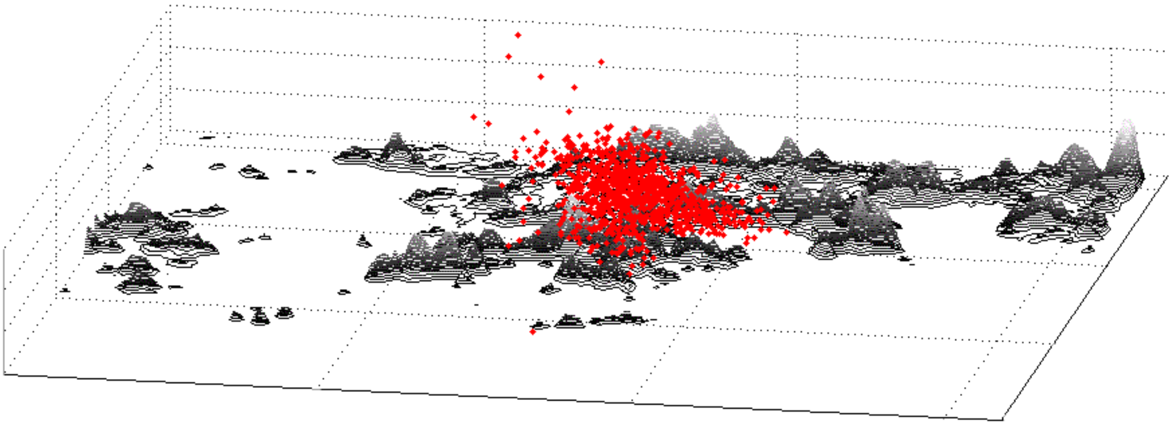

Figure 3 A sample output of the 3-dimensional dispersion of particles over terrain

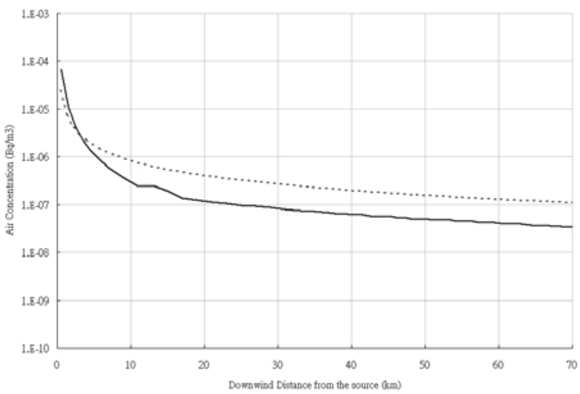

(a) Category B, 2 m/s

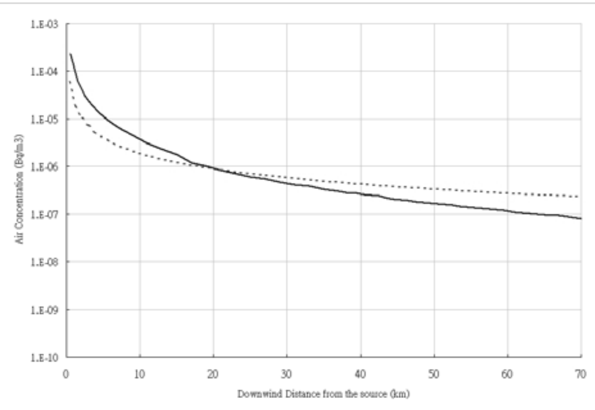

(b) Category D, 2 m/s

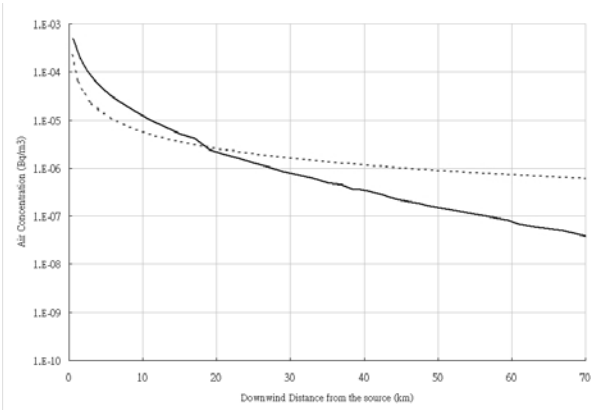

(c) Category F, 2 m/s

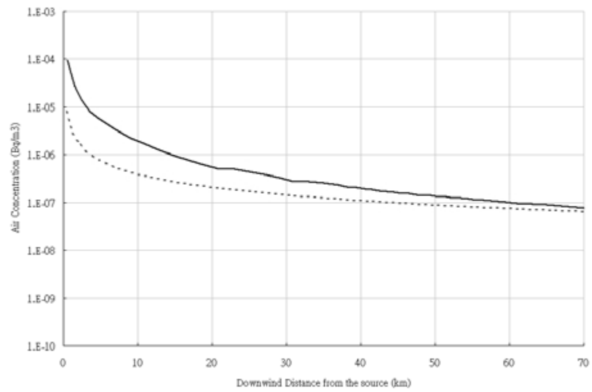

(d) Category D, 5 m/s

Figure 4 24-hour integrated air concentration (Bq/m^3) simulated by PDM and by ACAS along the plume centreline. [Solid line: ACAS; dotted line: PDM]

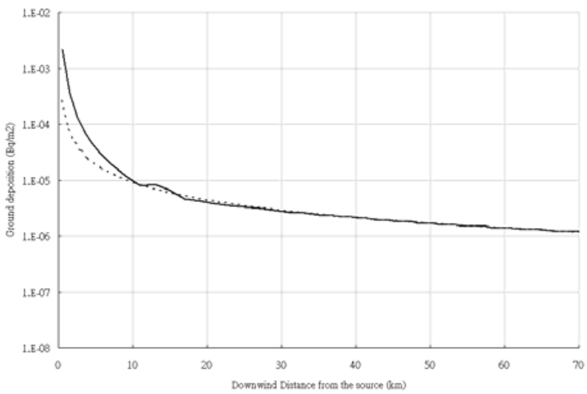

(a) Category B, 2 m/s

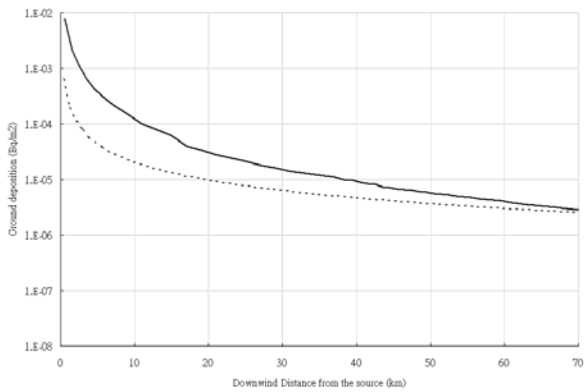

(b) Category D, 2 m/s

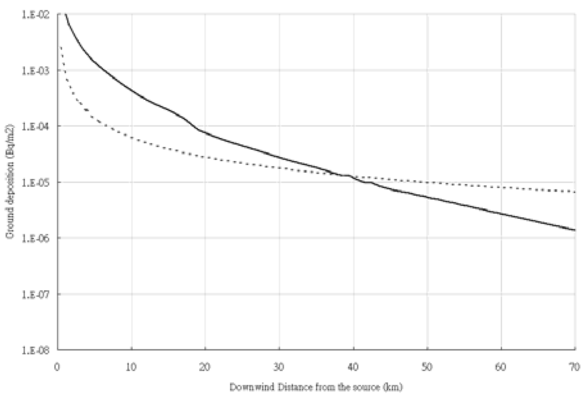

(c) Category F, 2 m/s

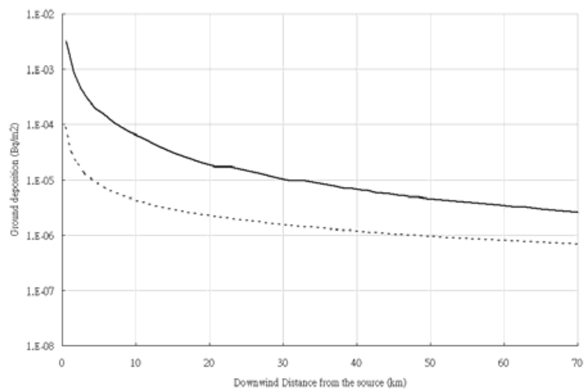

(d) Category D, 5 m/s

Figure 5 24-hour integrated ground deposition (Bq/m^2) simulated by PDM and by ACAS along the plume centreline. [Solid line: ACAS; dotted line: PDM]

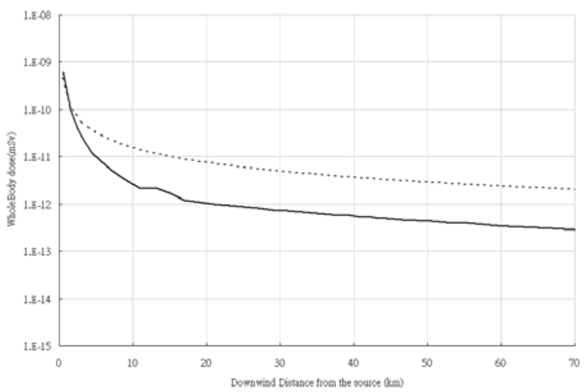

(a) Category B, 2 m/s

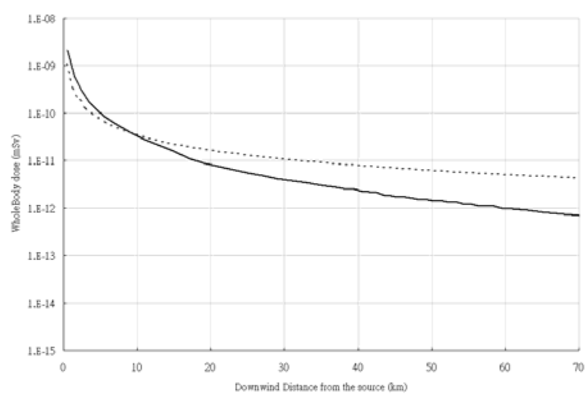

(b) Category D, 2 m/s

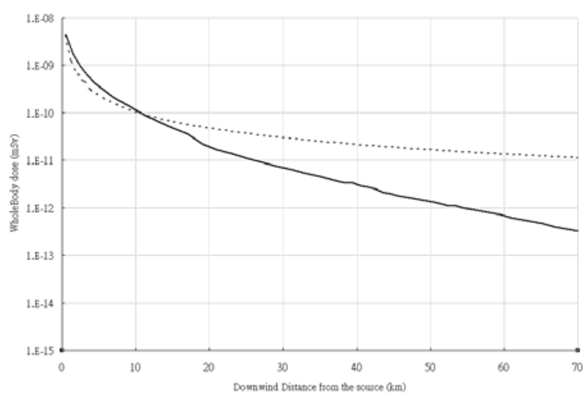

(c) Category F, 2 m/s

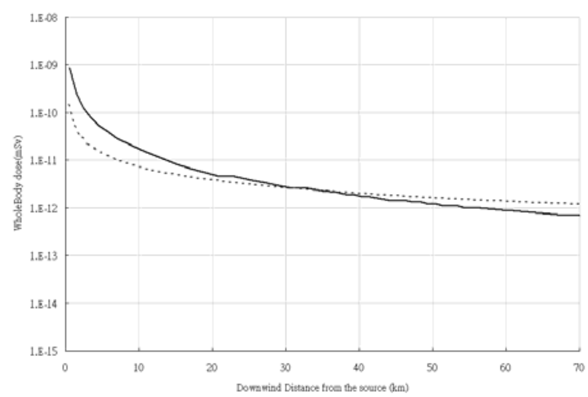

(d) Category D, 5 m/s

Figure 6 24-hour integrated whole body dose (mSv) simulated by PDM and by ACAS along the plume centreline. [Solid line: ACAS; dotted line: PDM]

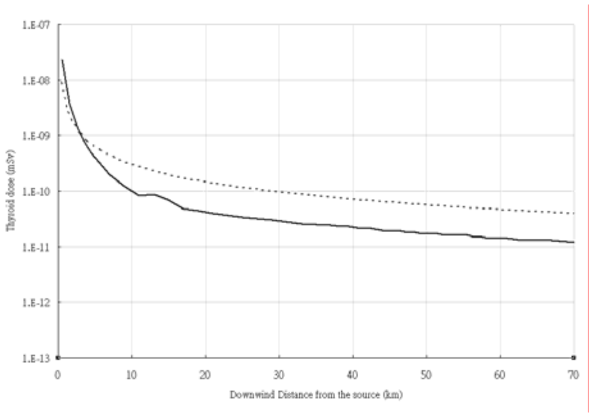

(a) Category B, 2 m/s

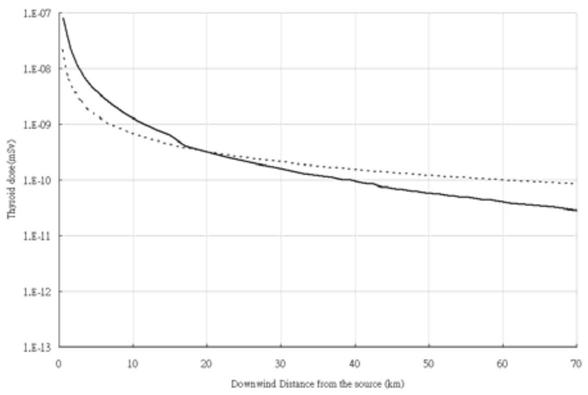

(b) Category D, 2 m/s

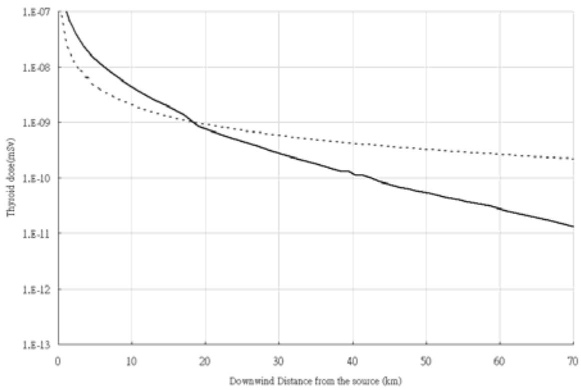

(c) Category F, 2 m/s

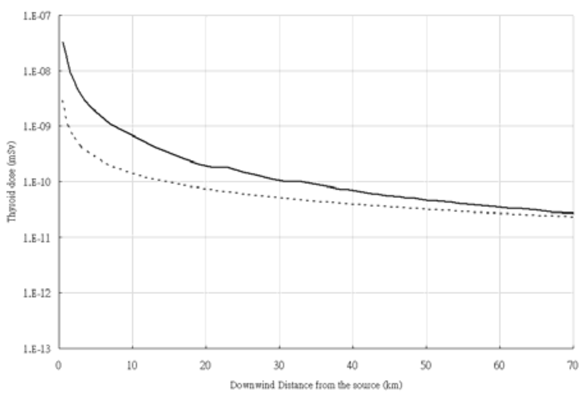

(d) Category D, 5 m/s

Figure 7 24-hour integrated thyroid dose (mSv) simulated by PDM and by ACAS along the plume centreline. [Solid line: ACAS; dotted line: PDM]

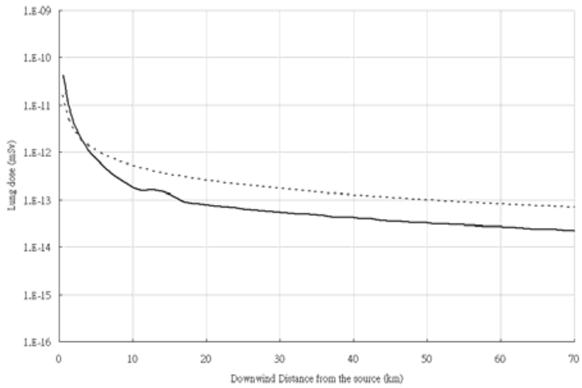

(a) Category B, 2 m/s

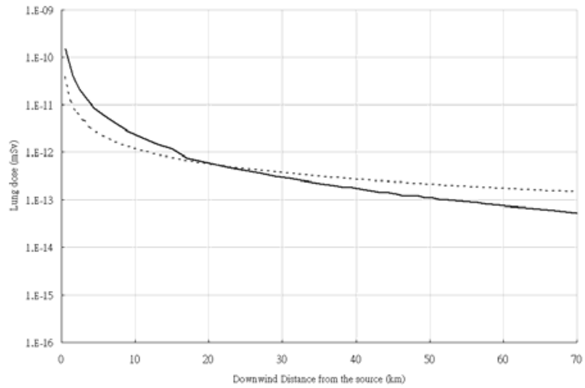

(b) Category D, 2 m/s

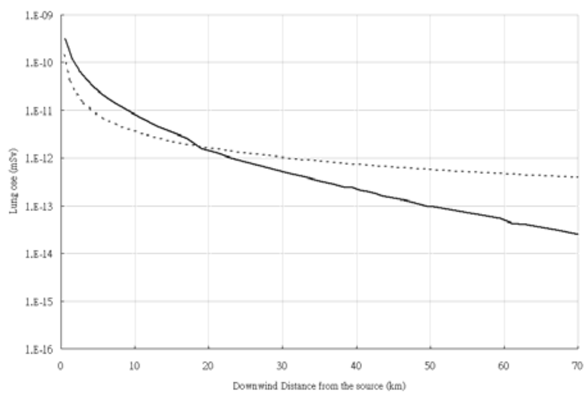

(c) Category F, 2 m/s

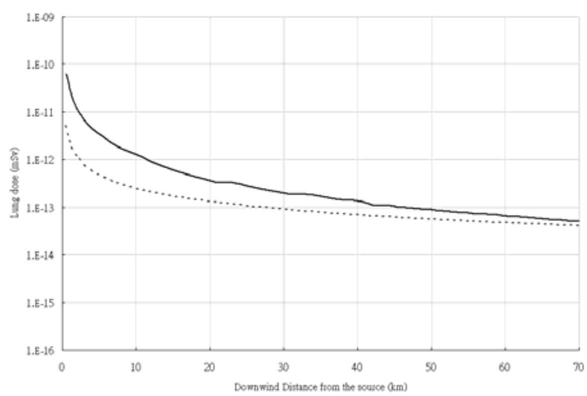

(d) Category D, 5 m/s

Figure 8 24-hour integrated lung dose (mSv) simulated by PDM and by ACAS along the plume centreline. [Solid line: ACAS; dotted line: PDM]

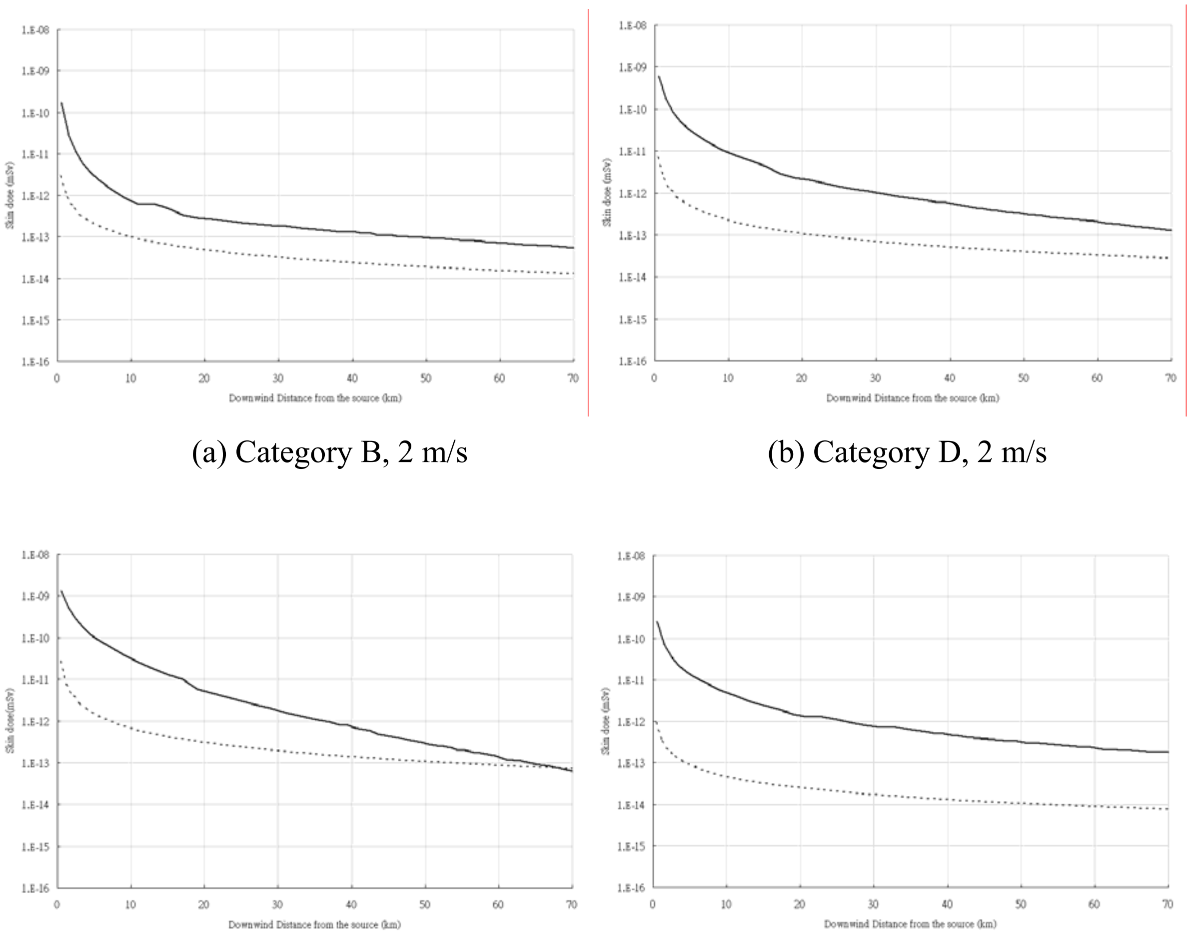

(a) Category B, 2 m/s

(b) Category D, 2 m/s

(c) Category F, 2 m/s

(d) Category D, 5 m/s

Figure 9 24-hour integrated skin dose (mSv) simulated by PDM and by ACAS along the plume centreline. [Solid line: ACAS; dotted line: PDM]

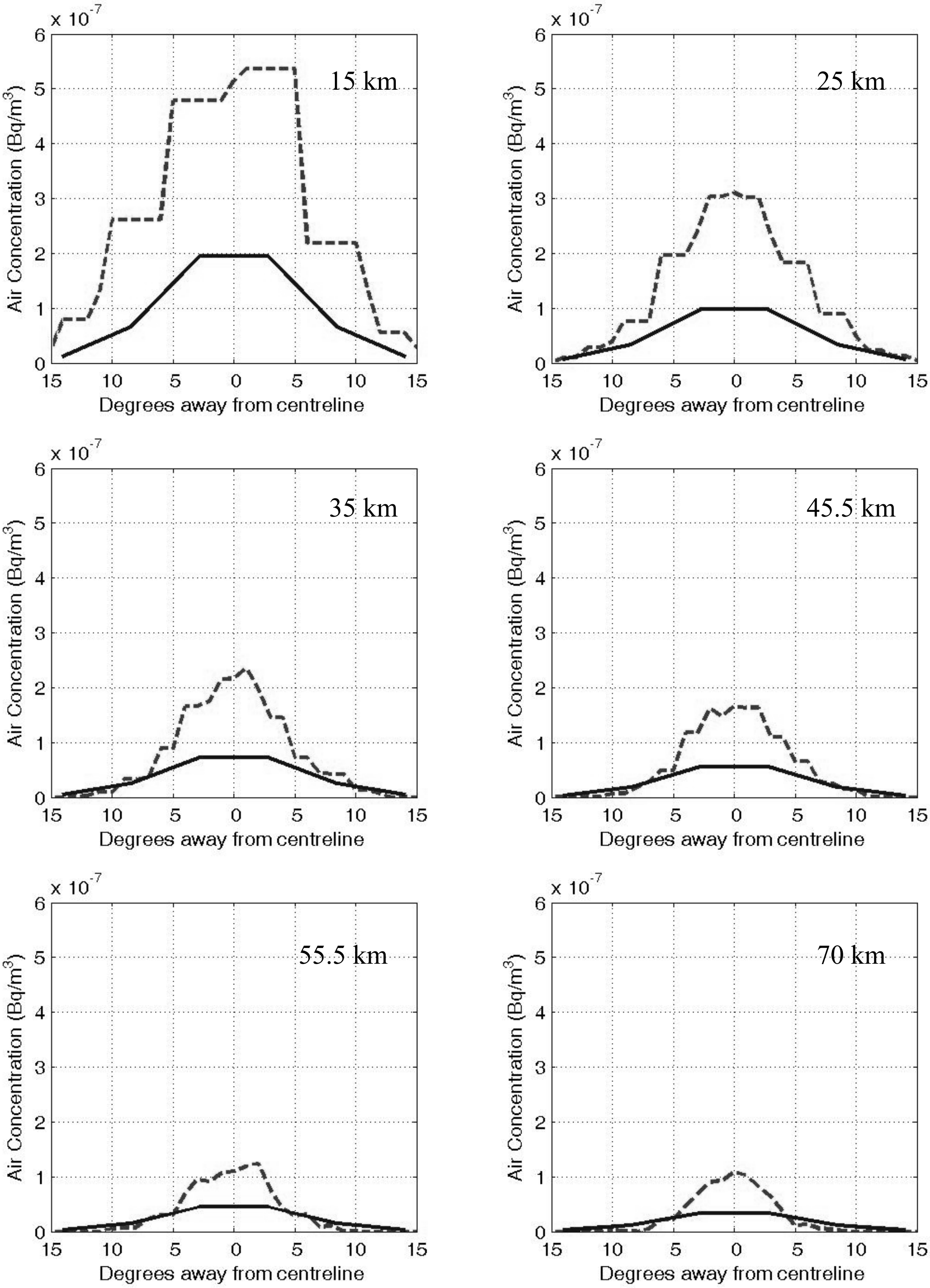

Figure 10 Cross-wind profiles of 24-hour integrated air concentration (Bq/m^3) simulated by PDM (dotted) and by ACAS (solid) at different downwind distances [Stability Category B (very unstable) at 2 m/s wind speed]

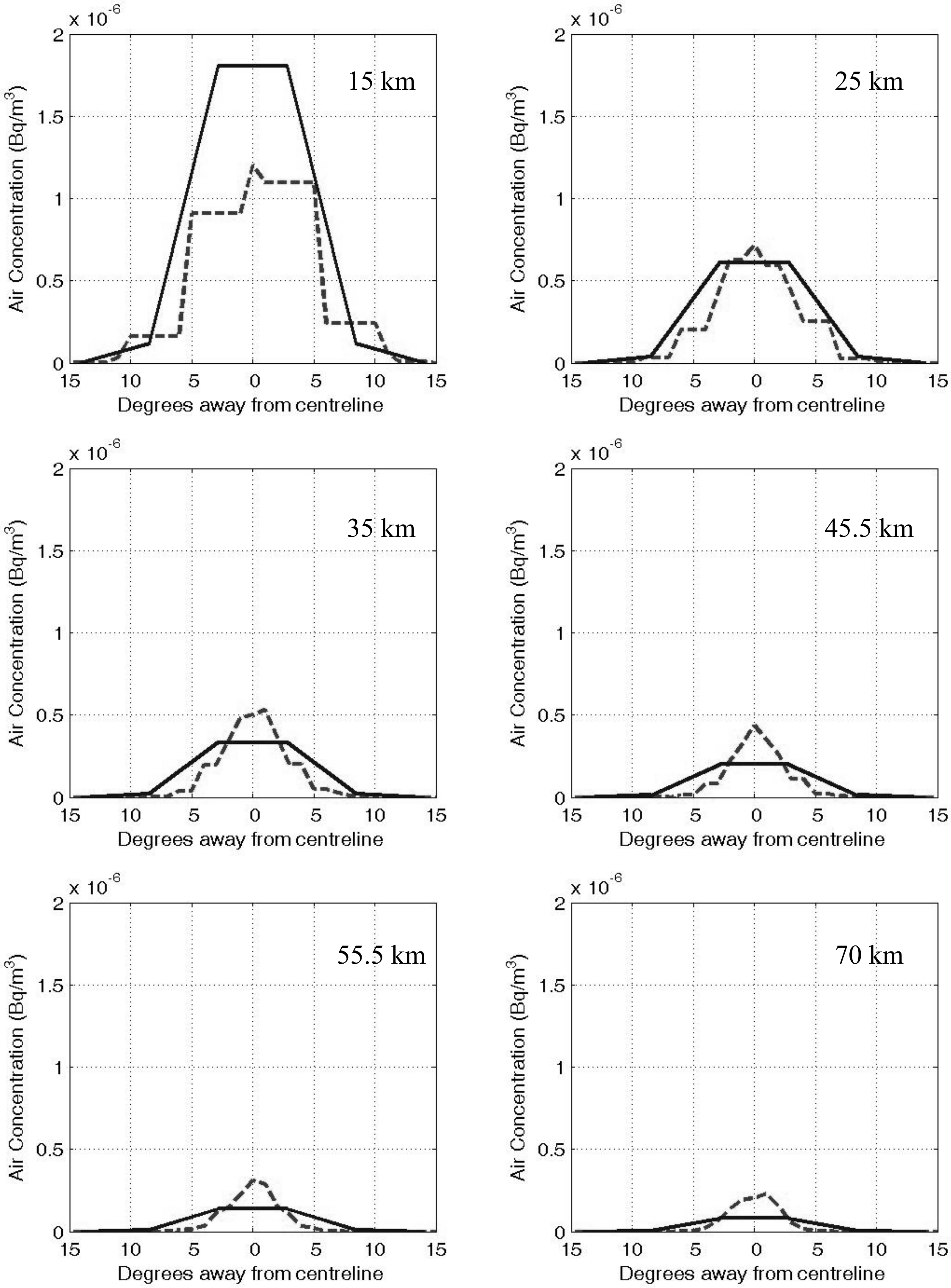

Figure 11 Cross-wind profiles of 24-hour integrated air concentration (Bq/m^3) simulated by PDM (dotted) and by ACAS (solid) at different downwind distances [Stability Category D (neutral) at 2 m/s wind speed]

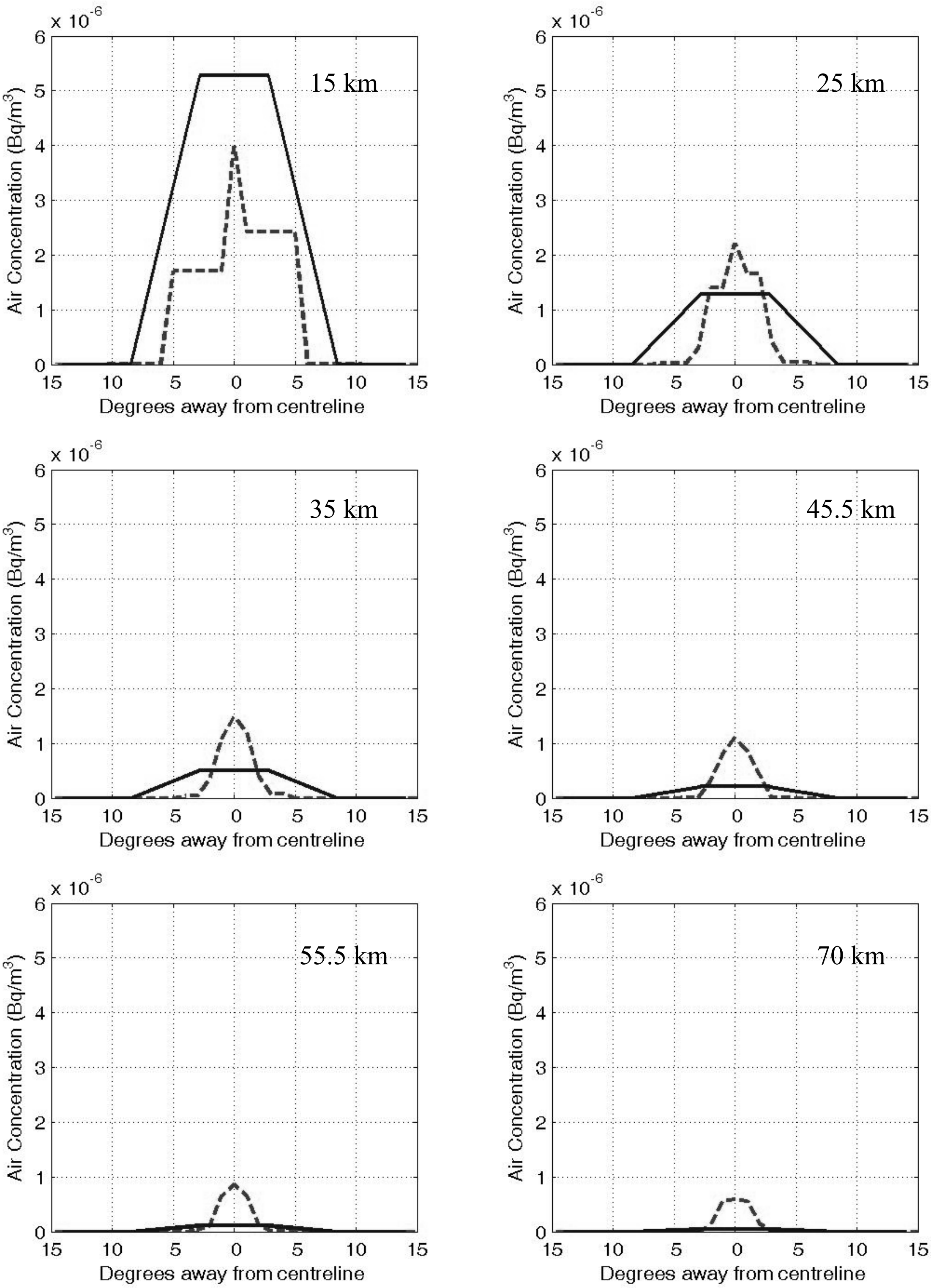

Figure 12 Cross-wind profiles of 24-hour integrated air concentration (Bq/m^3) simulated by PDM (dotted) and by ACAS (solid) at different downwind distances [Stability Category F (very stable) at 2 m/s wind speed]

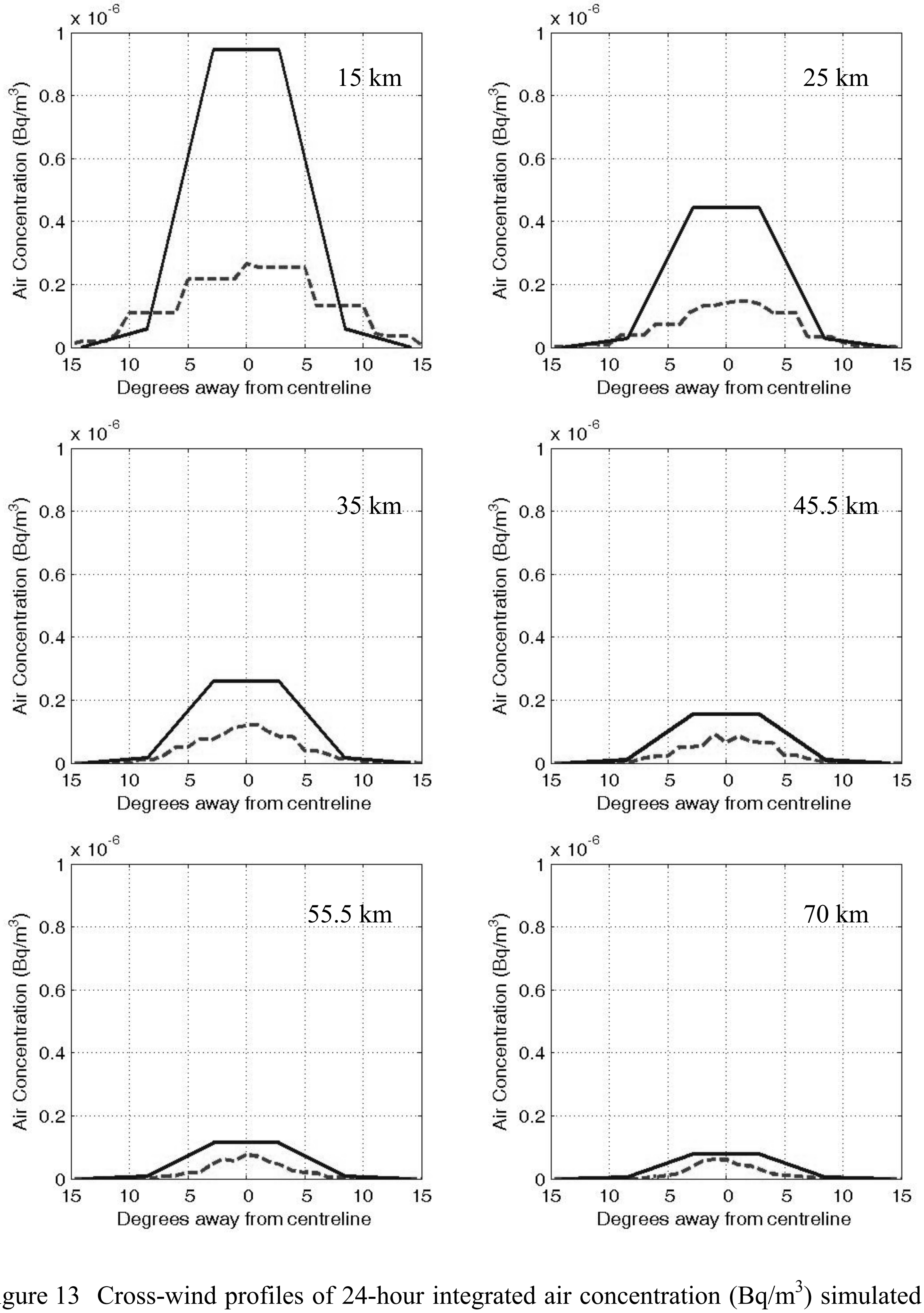

Figure 13 Cross-wind profiles of 24-hour integrated air concentration (Bq/m^3) simulated by PDM (dotted) and by ACAS (solid) at different downwind distances [Stability Category D (neutral) at 5 m/s wind speed]

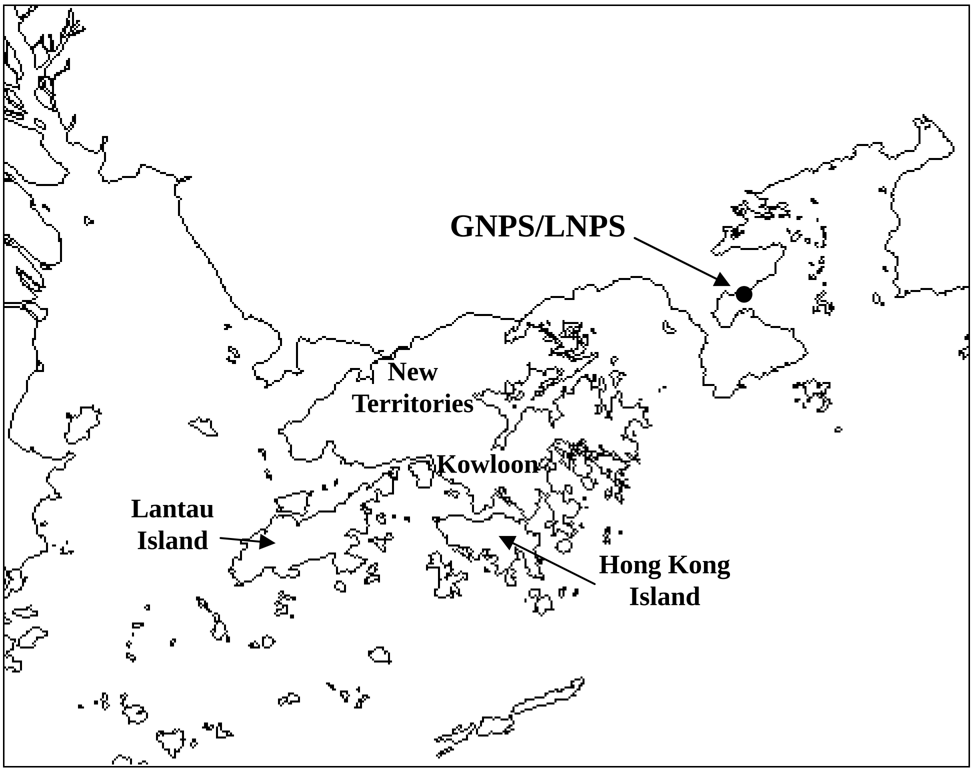

Figure II-1 Location of GNPS/LNPS and simulation domain of PDM

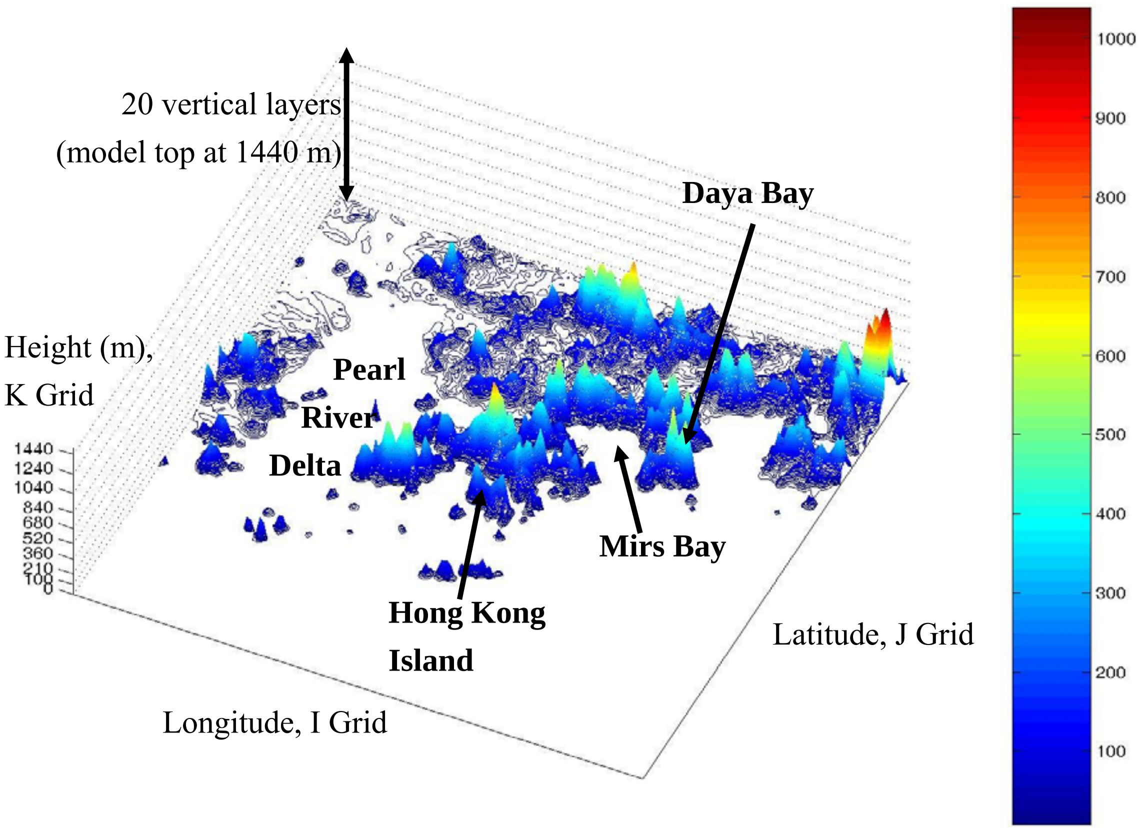

Figure II-2 Three-dimensional terrain elevation (in metres) for the PDM domain